

Lecture 18: NSOM imaging of optoelectronic devices & films

- Briefs of optoelectronic devices, and central research (debate) of optoelectronic devices: properties and processes.
- Advantages of NSOM imaging when applied to film materials, which dominate the current organic optoelectronic devices.
- Different operation modes of NSOM imaging and several examples:
 1. Organic solar cells: local nanostructure and photoconversion relationship
 2. Polymer dispersed liquid crystals;
 3. Conjugate polymer films;
 4. Bi-block polymer films;
 5. Dendrimer films;

Optoelectronic devices (materials)

- Optoelectronic materials are both **optical** and **electrical** active.
 1. **Optical** --- strong absorption and/or emission, polarization, or non-linear optical properties;
 2. **Electrical** --- high efficiency for light-to-electricity conversion (photovoltaic), or electricity-to-light conversion (electroluminescence).
 - Optoelectronic materials can be organic or inorganic semiconductors, or even metals (nanocrystal state, e.g. silver nanoparticle (prism, rod) as non-linear optical materials, see George Schatz work at NW).
 - Organic semiconductor has now attracted more interests in development of optoelectronic devices, due to the vast options of organic molecular structures --- covering the whole visible spectrum and can be tuned to be both **n-** and **p-**type semiconductors.
 - The recently developed microscopic and spectroscopic techniques has enabled the measurement at higher resolution, thus helping understanding the basic properties and processes of optoelectronic materials.
-

Some review papers on organic optoelectronic materials

Nature Materials, VOL 2, 2003, p641

NEWS & VIEWS

ORGANIC SEMICONDUCTORS

An equal-opportunity conductor

Until now, organic semiconductors, such as pentacene, have only allowed the flow of one type of charge. A new study confirms that—like their inorganic counterparts—both positive and negative charges can flow in the same material.

HENNING SIRRINGHAUS is at the Cavendish Laboratory, University of Cambridge, Cambridge CB3 0HE, UK. e-mail: h.sirringhaus@cam.ac.uk

Conjugated organic polymers and molecules exhibit semiconducting properties, which are in many respects similar to those of inorganic semiconductors and make them suitable for use in practical electronic devices, such as light-emitting and photovoltaic diodes and field-effect transistors. In contrast to many inorganic semiconductors, however, organic semiconductors (OSC) do not commonly display ambipolar charge transport of both positive holes and negative electrons that would enable the fabrication of complementary CMOS-type transistor circuitry using a single OSC material. On page 678 of this issue, Meijer *et al.* demonstrate that ambipolar conduction is in fact a generic feature of OSCs.

In a thin-film transistor (TFT), a voltage is usually applied to the gate electrode, which is separate from the semiconductor layer by a thin dielectric (Fig. 1a). The gate voltage causes the formation of a thin layer of accumulated charge at the semiconductor–dielectric interface, and results in an increase in current flow between two charge-injecting electrodes known as the source and drain. Most OSCs are p-type— that is, the application of a negative gate voltage results in formation of an accumulation layer of positive hole carriers. Reversing the polarity of the gate voltage should create an 'inversion' layer of negative electrons, but this is not usually observed in OSC transistors.

There are at least two possible reasons for this lack of ambipolar behaviour. First, it is difficult to engineer the metallic source and drain electrodes to simultaneously provide efficient charge injection for both electrons and holes into the OSC. An OSC has molecular orbitals, which are analogous to the valence- and conduction-band edges in an inorganic semiconductor. The lower energy orbitals are called the highest occupied molecular orbital (HOMO) level, and the higher-energy orbital forms the lowest unoccupied molecular orbital (LUMO) level (Fig. 1b). The HOMO and LUMO are

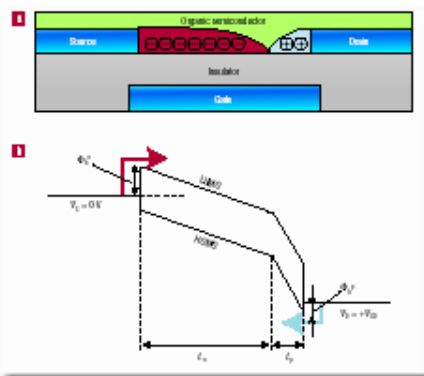


Figure 1 Most semiconductors can charge transport flow both ways in an organic semiconductor (OTFT). For the system studied by Meijer *et al.*, the transistor is a *p*-channel structure of an organic thin-film transistor (TFT). The energy level profile in the organic TFT before the gate voltage V_G is low, so that the source–drain voltages, V_D , such that the electrical field across the gate electrode changes sign at some point in the channel. The region of the channel near the drain electrode (length L_D) exhibits *p*-type carrier (hole) injection, and the region near the drain electrode (length L_S) exhibits *n*-type carrier (electron) injection. The energy barriers for injection of electrons and holes at the respective contacts, ϕ_{n2} and ϕ_{p1} , are also shown.

separated by an energy gap, similar to the bandgap in an inorganic semiconductor.

For efficient hole injection into the OSC, a metallic material such as gold is chosen with a work function that closely matches the HOMO level of the semiconductor.

Chem. Mater. 2004, 16, 4436–4451

Introduction to Organic Thin Film Transistors and Design of n-Channel Organic Semiconductors

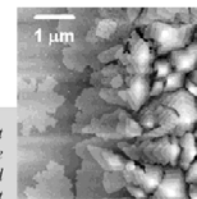
Christopher R. Newman,[‡] C. Daniel Frisbie,^{*,‡} Demetrio A. da Silva Filho,[§] Jean-Luc Brédas,[§] Paul C. Ewbank,[†] and Kent R. Mann[‡]

Departments of Chemistry and of Chemical Engineering and Materials Science, University of Minnesota, Minneapolis, Minnesota 55455, and School of Chemistry and Biochemistry, Georgia Institute of Technology, Atlanta, Georgia 30332

ADVANCED MATERIALS

Organic Thin Film Transistors for Large Area Electronics

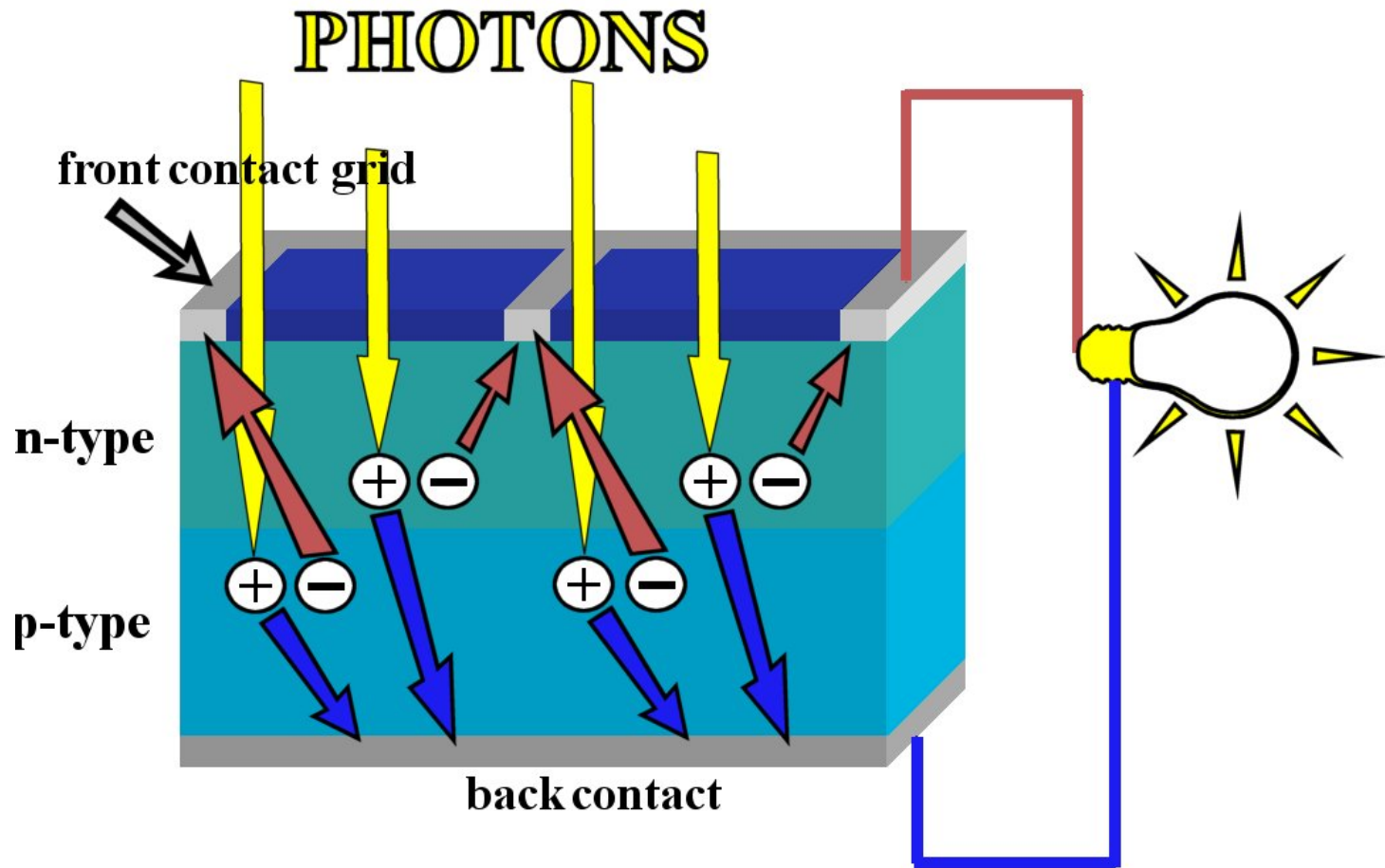
By Christos D. Dimitrakopoulos* and Patrick R. L. Malenfant



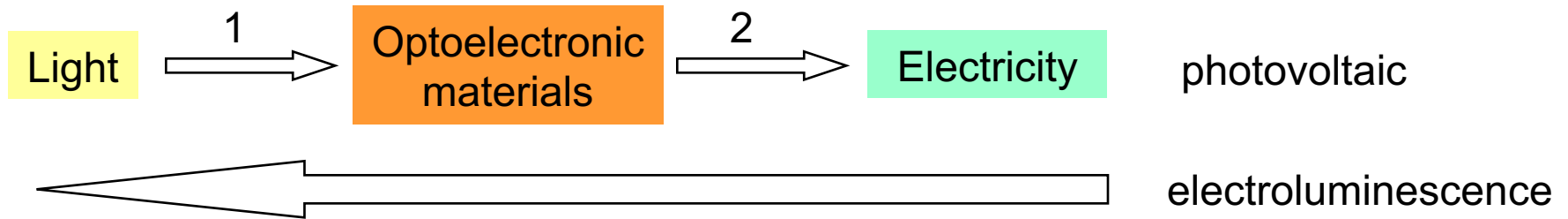
Organic thin-film transistors (OTFTs) have lived to see great improvements in recent years. This review presents new insight into conduction mechanisms and performance characteristics, as well as opportunities for modeling properties of OTFTs. The shifted focus in research from novel chemical structures to fabrication technologies that optimize morphology and structural order is underscored by chapters on vacuum-deposited and solution-processed organic semiconducting films. Finally, progress in the growing field of the *n*-type OTFTs is discussed in ample detail. The Figure, showing a pentacene film edge on SiO₂, illustrates the morphology issue.

Adv. Mater. 2002, 14, p99.

Scheme of a solar cell

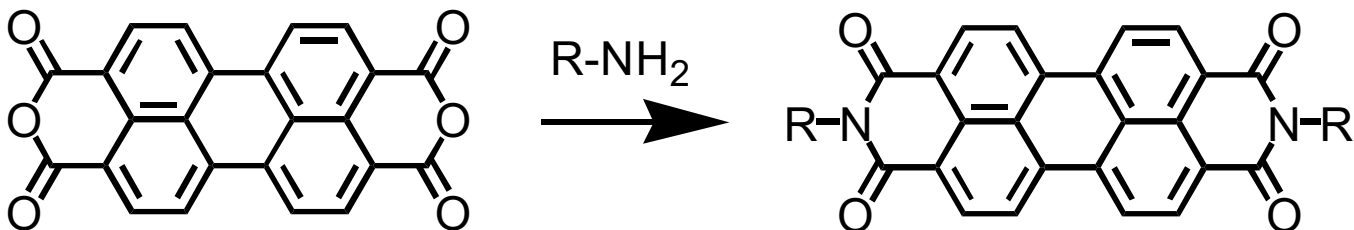


Central debates of optoelectronic materials



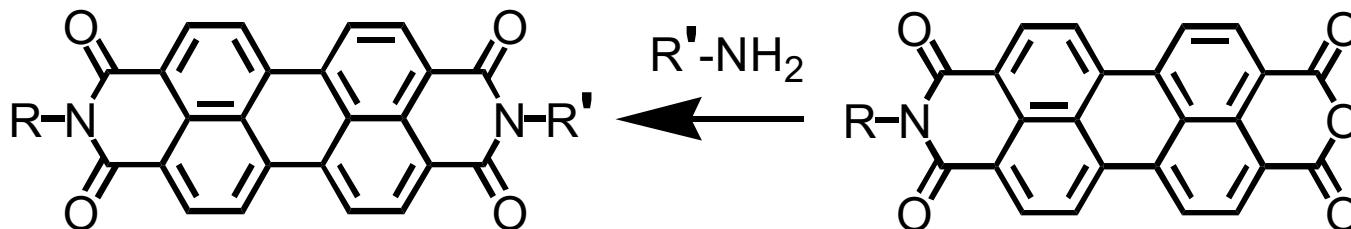
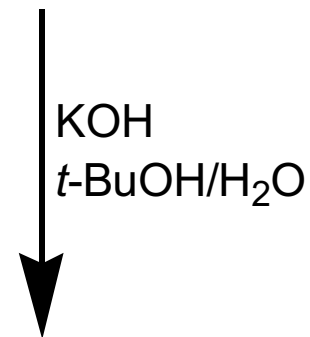
- Mechanism: electrical excitation \rightarrow electron-hole recombination \rightarrow light emission, or the reverse.
- Performance of organic optoelectronic devices depends on **exciton (electron-hole pair) diffusion**, **exciton dissociation** at p-n junctions, **charge carrier mobility**, which in turn are all determined by the intermolecular interaction --- self-assembled nanostructures.
- Huge amount of **debates** and **conflict** concerned the similar device or even the same materials.
- For example, for the same material PTCDI (*see slide*), the charge carrier mobility has been measured in a wide range, from $\sim 10^{-5}$ to $\sim 1.0 \text{ cm}^2 \text{ V}^{-1} \text{ s}^{-1}$, and the exciton diffusion has been reported to be from **nm** to **μm** .
- While various organic materials and device structures have been developed and explored, the primary challenge is still to understand the fundamental **photoinduced processes** and **physical requirements** for improving the photoconversion, especially at microscopic or nanoscopic levels.

PTCDI molecules: *a n-type semiconductor*

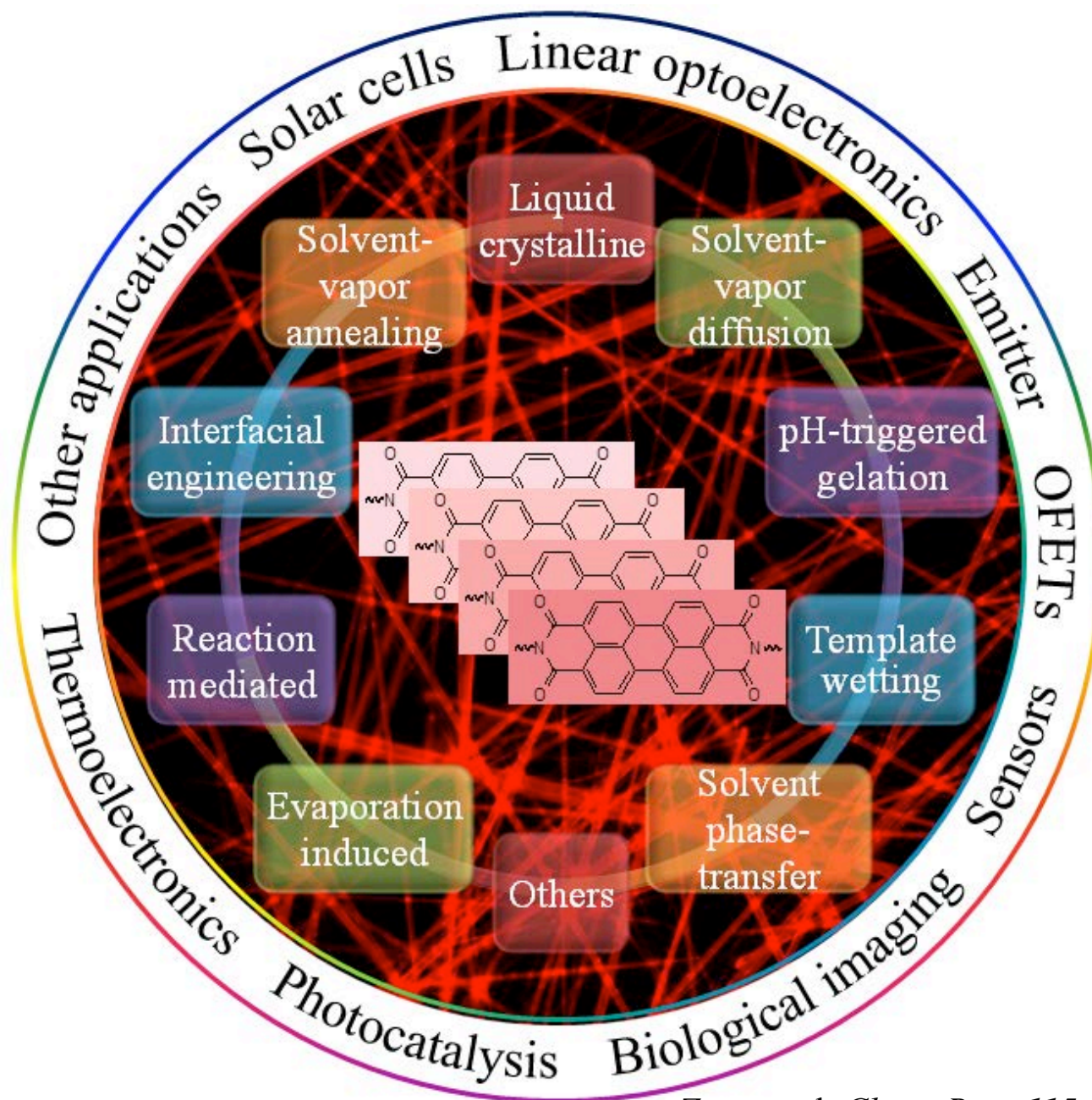


R = alkyl, aryl, polyoxyalkyl;

R' = functional moieties: amine,
carboxylic, thiol, etc.



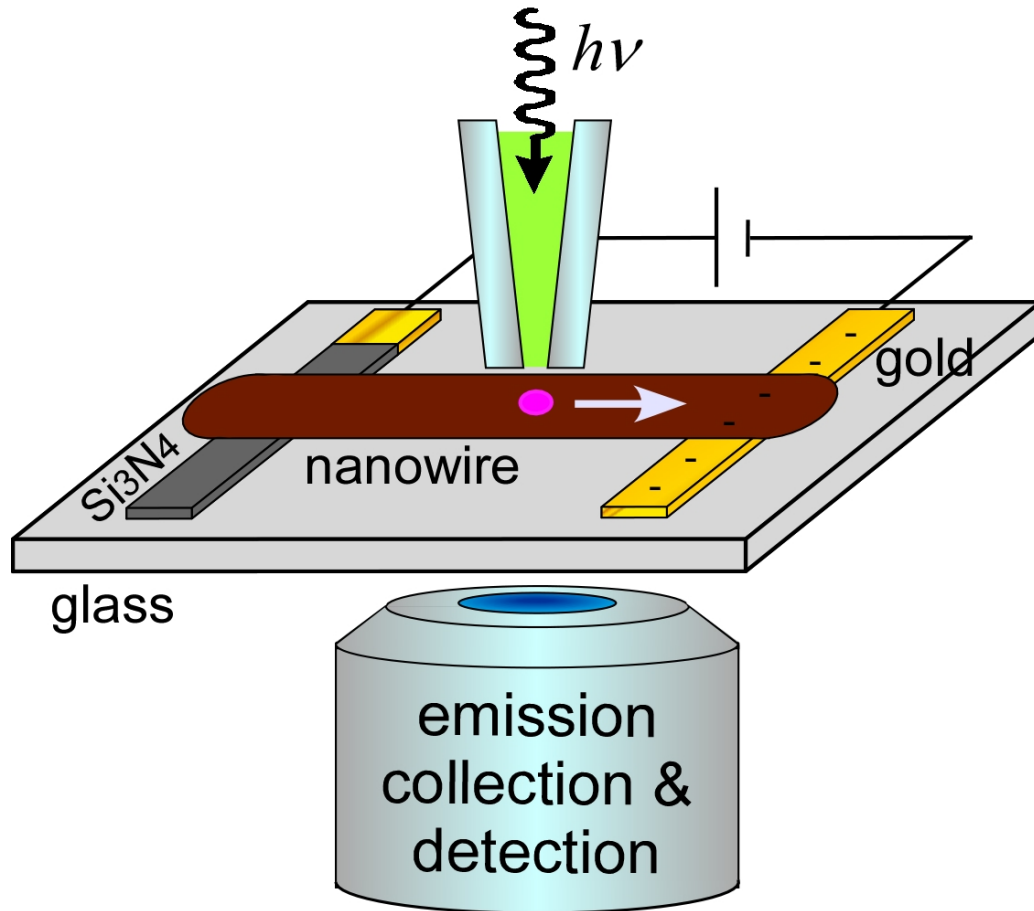
PTCDI: n-type semiconductor with wide applications



NSOM imaging of optoelectronic devices (materials)

- Major imaging modes for NSOM: emission (for **LED**) and bias modulation (for **photovoltaic devices**).
See scheme of local detection of emission, to be drawn on board.
- A combination of emission and bias modulation affords in situ investigation of photovoltaic devices --
- calibrating of solar cell materials.
- High spatial resolution --- revealing structure dependence of device performance; single-particle measurement pave the way for nanoelectronic devices (nanowires, nanorods ...).
- The ultra fine laser spot from NSOM tip provides highly local and precise excitation of small nanomotifs, like a nanowire. *See the slide.*
- Tunable with femtosecond **pulsed** laser system for ultrafast charge or energy transfer processes.
- Tunable with polarization systems for molecular packing structure, which determines both the charge mobility and exciton diffusion.
- Recently developed nanoscale spectrometry: **NSOM Raman** --- useful for addressing local optical properties and molecular interaction at interface (particularly at transition metal surface, which is often used as electrode in optoelectronic devices).

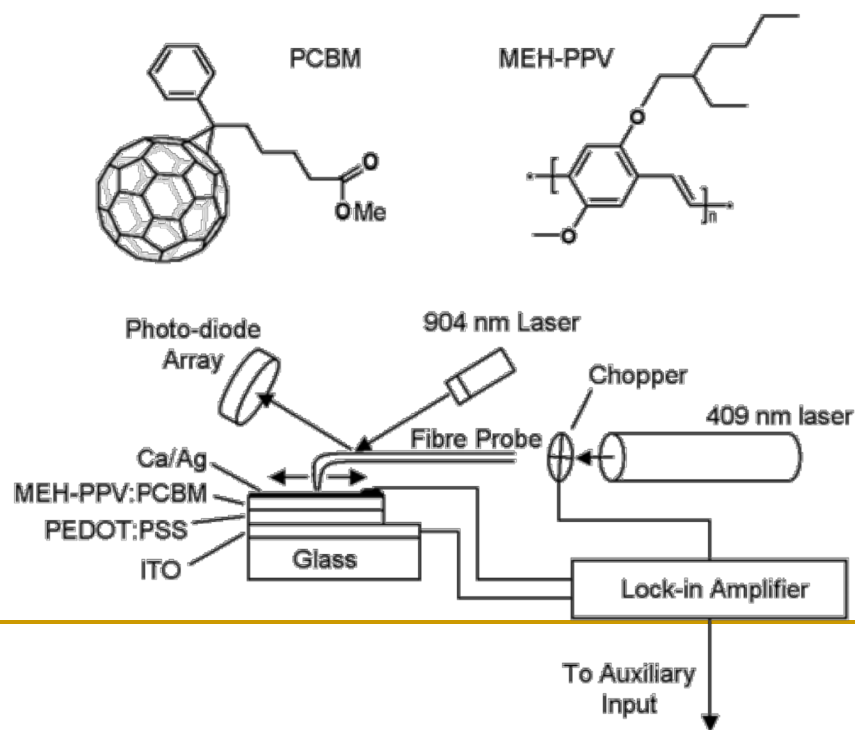
NSOM imaging of exciton diffusion in a nanowire



Direct Photocurrent Mapping of Organic Solar Cells Using a Near-Field Scanning Optical Microscope

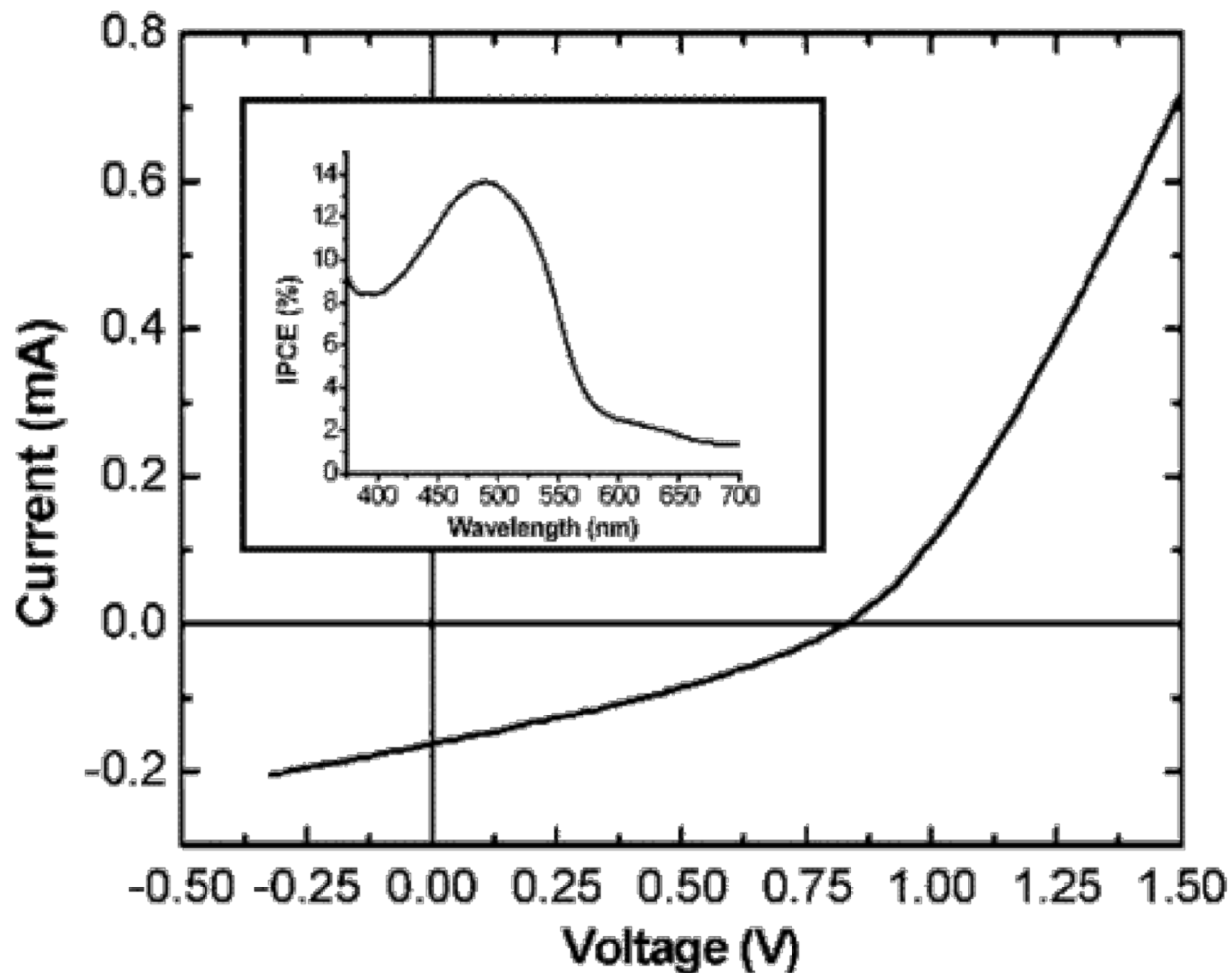
Christopher R. McNeill, Holger Frohne, John L. Holdsworth, John E. Furst, Bruce V. King, and Paul C. Dastoor*

*School of Mathematical and Physical Sciences, University of Newcastle,
University Drive, Callaghan, NSW, 2308 Australia*



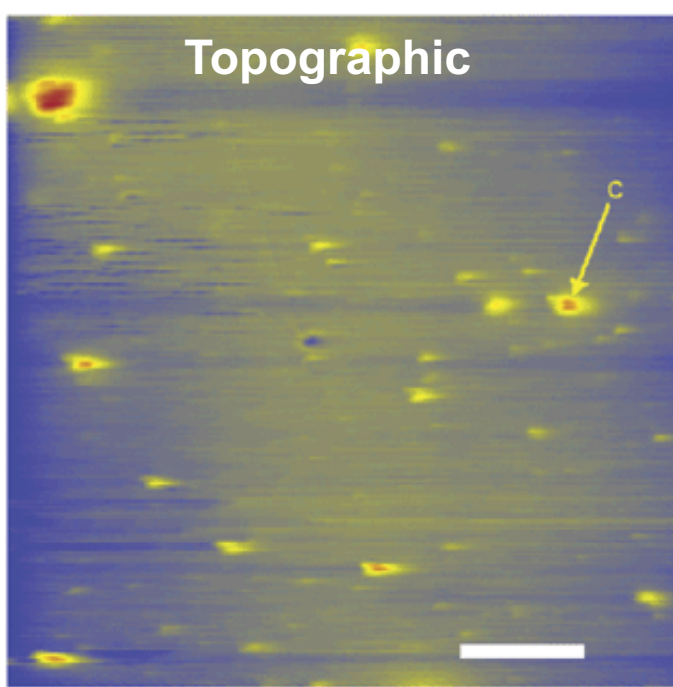
Research outline

- Direct photocurrent mapping of organic solar cells (OSCs) using a novel NSOM setup;
 - By raster scanning the light output from the NSOM across the OSC surface, it is possible to collect **height and photocurrent images simultaneously** with a high lateral resolution.
 - The photocurrent images demonstrate that film inhomogeneities and segregation effects strongly influence OSC device performance.
-



Far-field current-voltage characteristics of the ITO/PEDOT-PSS/MEH-PPV-PCBM/Ca/Ag devices fabricated under 4 mW 532 nm illumination.

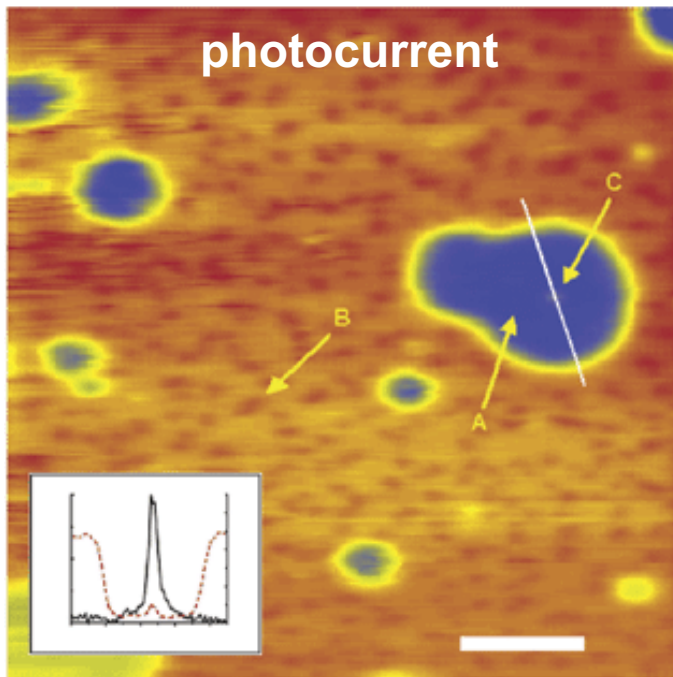
Inset: Corresponding incident photon collected electron (IPCE) efficiency spectra.



Topographic and current images of an ITO/PEDOT-PSS/MEH-PPV-PBCM/Ca/Ag device.

Two main features are observed:
large dark regions (marked A);
small bright regions (marked B).

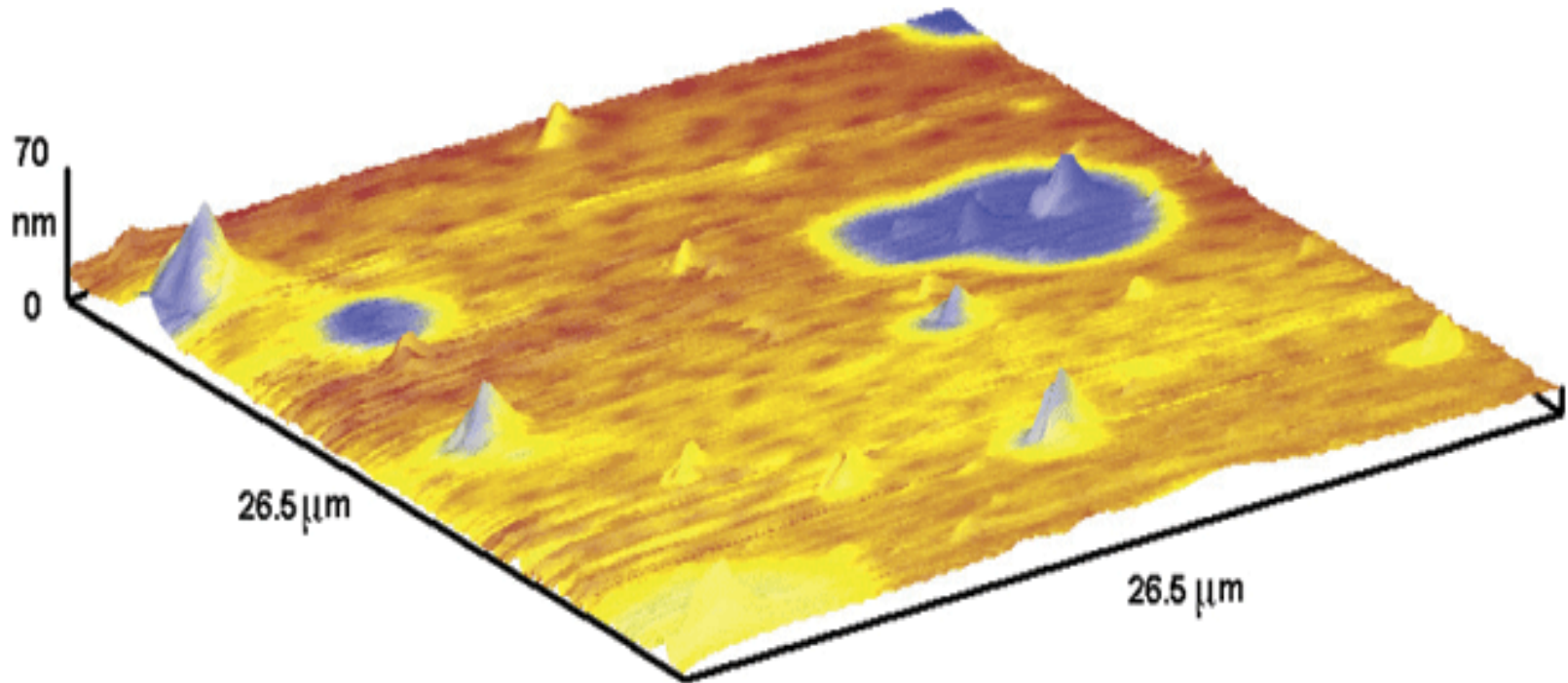
The feature marked C corresponds to a small bright feature in the center of the large dark region (A).



The inset shows the height (black, solid) and **current (red, dotted)** traces taken along the white line. The scale bar is 5 μm in length.

4D mapping of solar cell thin film

(3D topography + 4th D on current marked in color code)

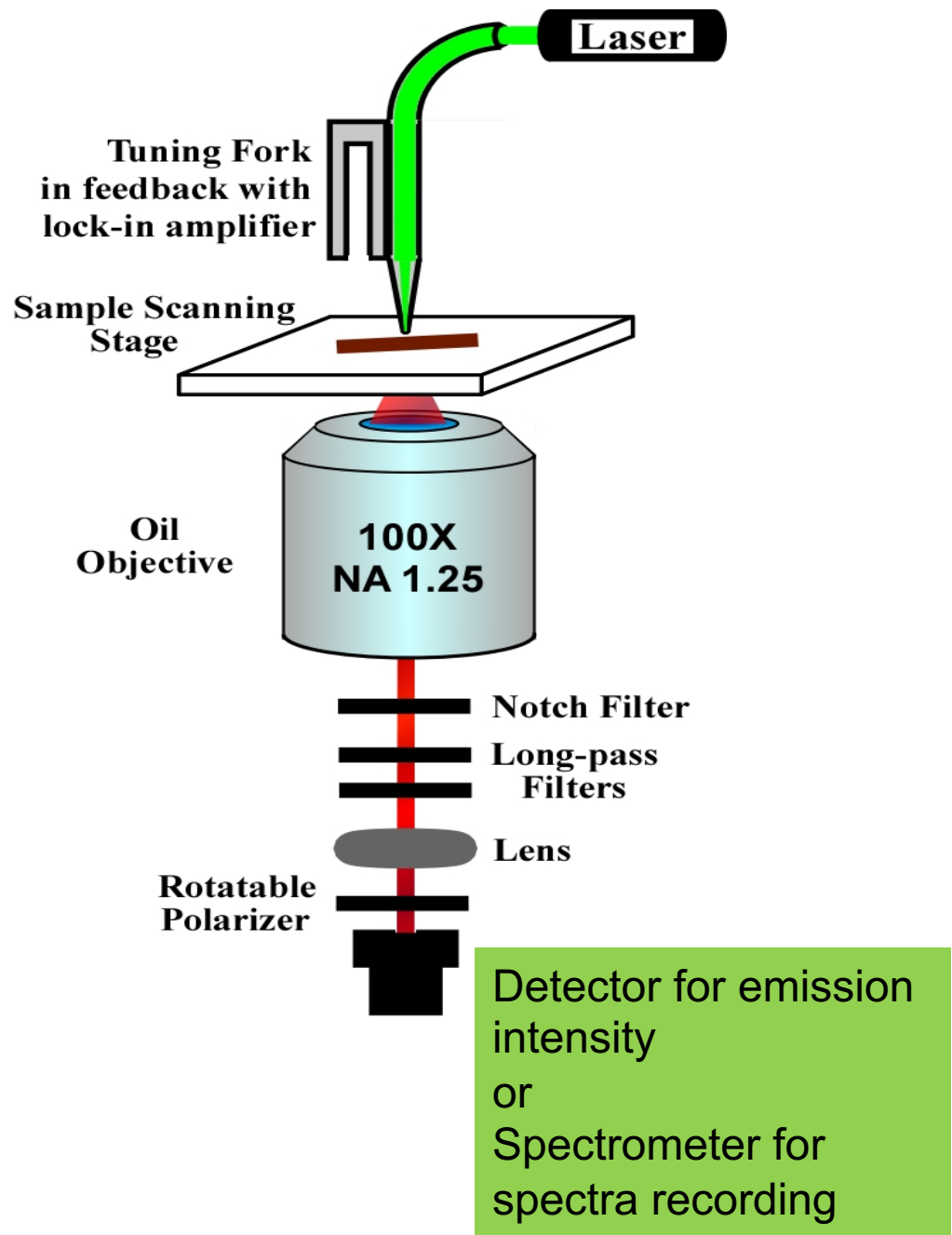


Composite 3D image of the **height** and **current** map images.

Red → higher current;

Blue → low current.

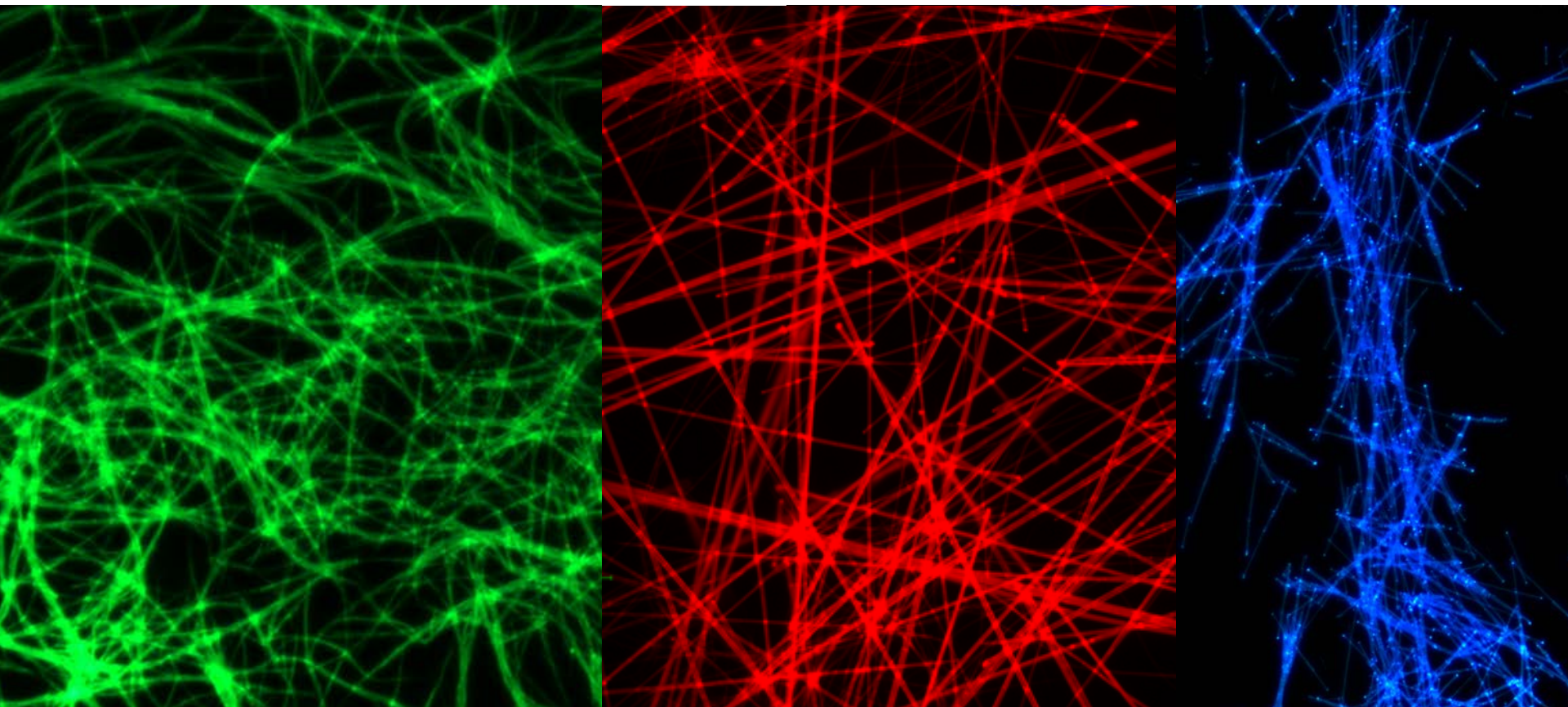
Extended NSOM system for multimode imaging and spectroscopy measurements



Advantages of NSOM imaging of film structures and properties

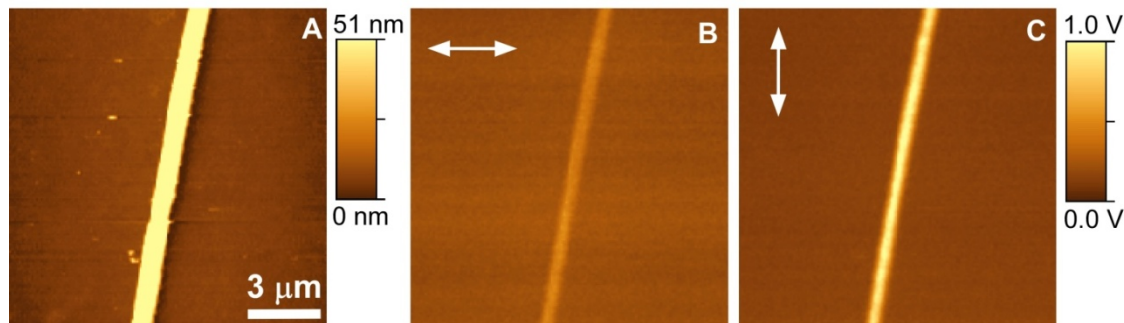
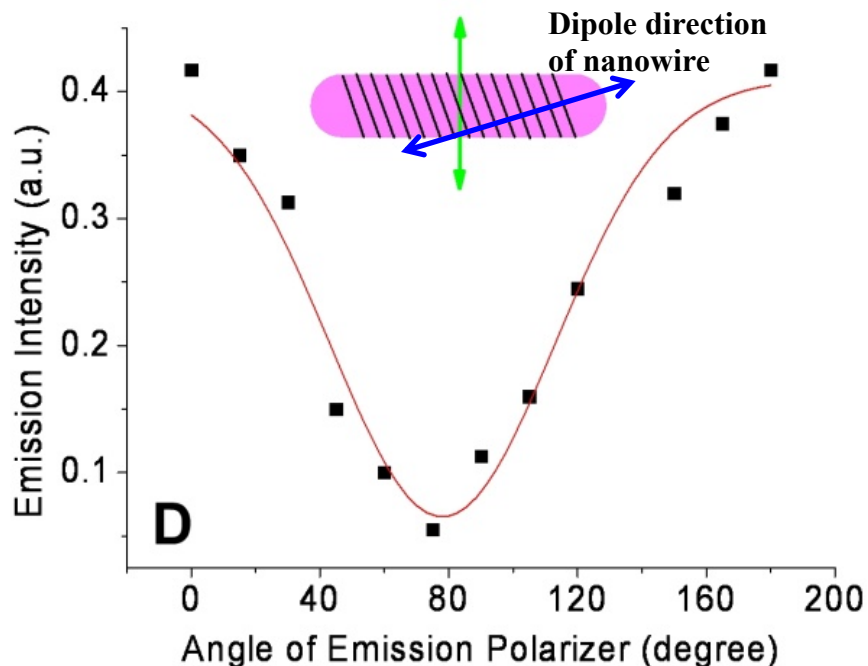
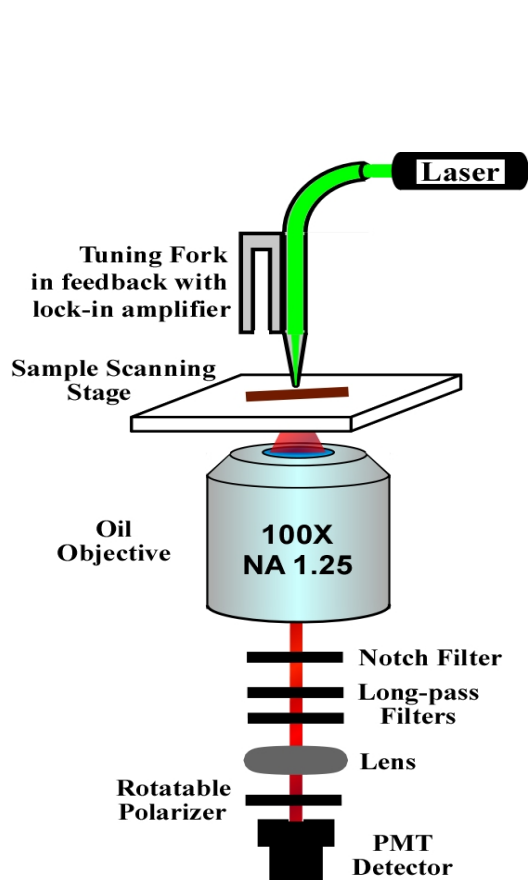
- Revealing the **heterogeneous structure** (distribution) of mixed films (e.g. polymer blends) --- transmissivity, emission intensity (different location), emission wavelength (different component), Raman scattering (surface vs. bulk). All these cannot be revealed using only AFM height measurement or optical microscopes.
- Direct correlation between local structure and spectroscopy properties --- e.g., quantum size effect for nanoparticles, local environment effect of proteins/enzymes.
- High spatial resolution --- mesoscopic investigation of films or devices. Nanoscopic organization is critical for charge migration and energy transport.
- Tunable for time resolved studies and polarization measurement --- crucial for photonic materials.
- Feasible for bias modulation --- applying a voltage between the tip and substrate.

Strong, tunable fluorescent emission in nanofibers



L. Zang et al., *Accounts of Chemical Research*, **41** (2008) 1596-1608
L. Zang et al. *Chem. Rev.*, **115** (2015) 11967-11998
Ling Zang, *Accounts of Chemical Research*, **48** (2015) 2705-2714

Linear polarized emission from a nanowire under NSOM



(A) NSOM topography image of a nanobelt assembled from propoxyethyl-PTCDI; belt thickness is about 50 nm. (B, C) NSOM emission images collected (by PMT) after a polarizer at horizontal and vertical positions; (D) Emission intensity of a single nanobelt depending on the angle between the polarizer and the long-axis of nanobelt. The inset (cartoon) shows the tilted packing of molecules along the long-axis of the nanobelt. The polarizer is indicated as an arrow.

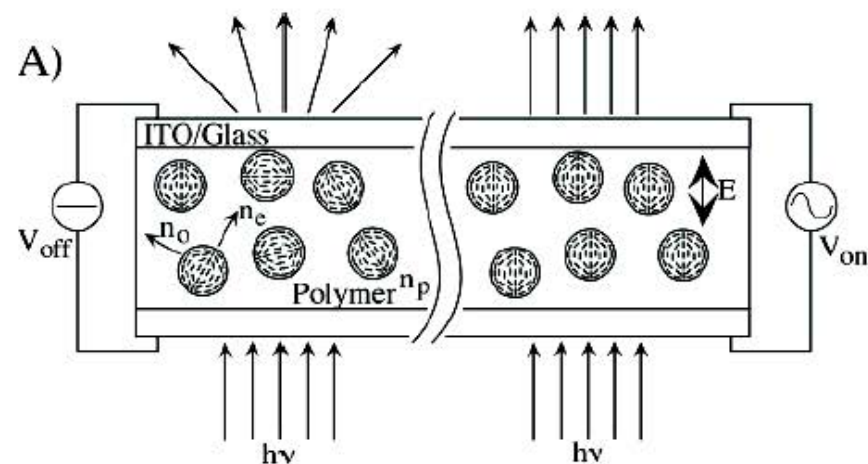
Different operation modes of NSOM imaging for different optical materials

- Transmission;
- Emission: collected by **objective** (backward vs. front face)
- Emission: collected by **tip** (normally excited at front face at an appropriate angle)
- Raman scattering: surface enhanced Raman scattering (SERS) on transition metals like Silver --- excitation via tip, collection via objective.

Optical Microscopy Studies of Dynamics within Individual Polymer-Dispersed Liquid Crystal Droplets

DANIEL A. HIGGINS,* JEFFREY E. HALL, AND AIFANG XIE

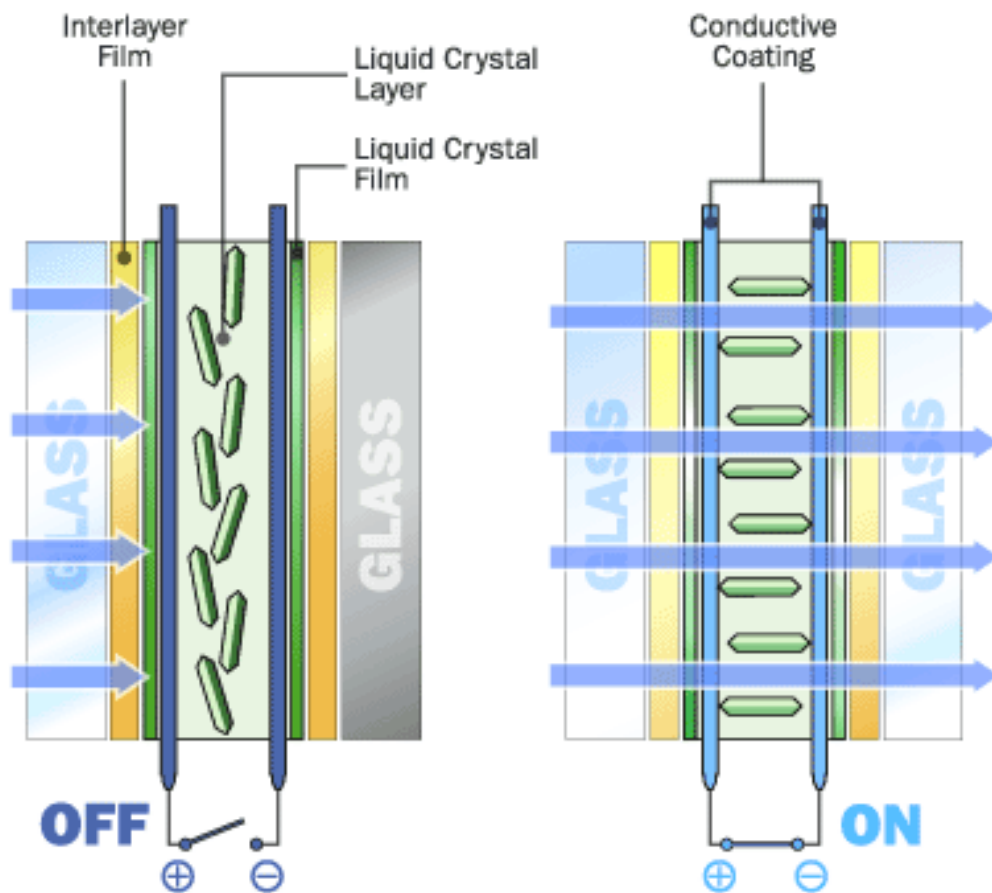
Department of Chemistry, Kansas State University, Manhattan, Kansas 66506



Polymer-dispersed liquid crystal (PDLC)

- PDLC thin films find a variety of applications in a range of optical devices.
- These include their use in electrically switchable (smart) windows, optical shutters, flexible displays, diffractive optics, and photorefractive systems.
- PDLCs consist of (sub)micrometer-sized birefringent LC droplets encapsulated within what is usually an **optically transparent polymer**.
- The molecular organization within the encapsulated LC droplets depends on the **elastic constants of the LC** and the interfacial anchoring conditions.
- In their native state, **the fast (or slow) optical axes** of these droplets are usually **randomly aligned**, causing the materials to **strongly scatter light**.
- When polymers and LCs with proper **refractive indices** are employed, application of an electric field causes the films to become optically transparent to normally incident light.
- This field-induced change results from reorientation of the LC directors within the droplets.

PDLC SMART WINDOWS



©2003 HowStuffWorks

An office cube with smart windows



An office cube with smart windows



An building with smart windows for energy saving

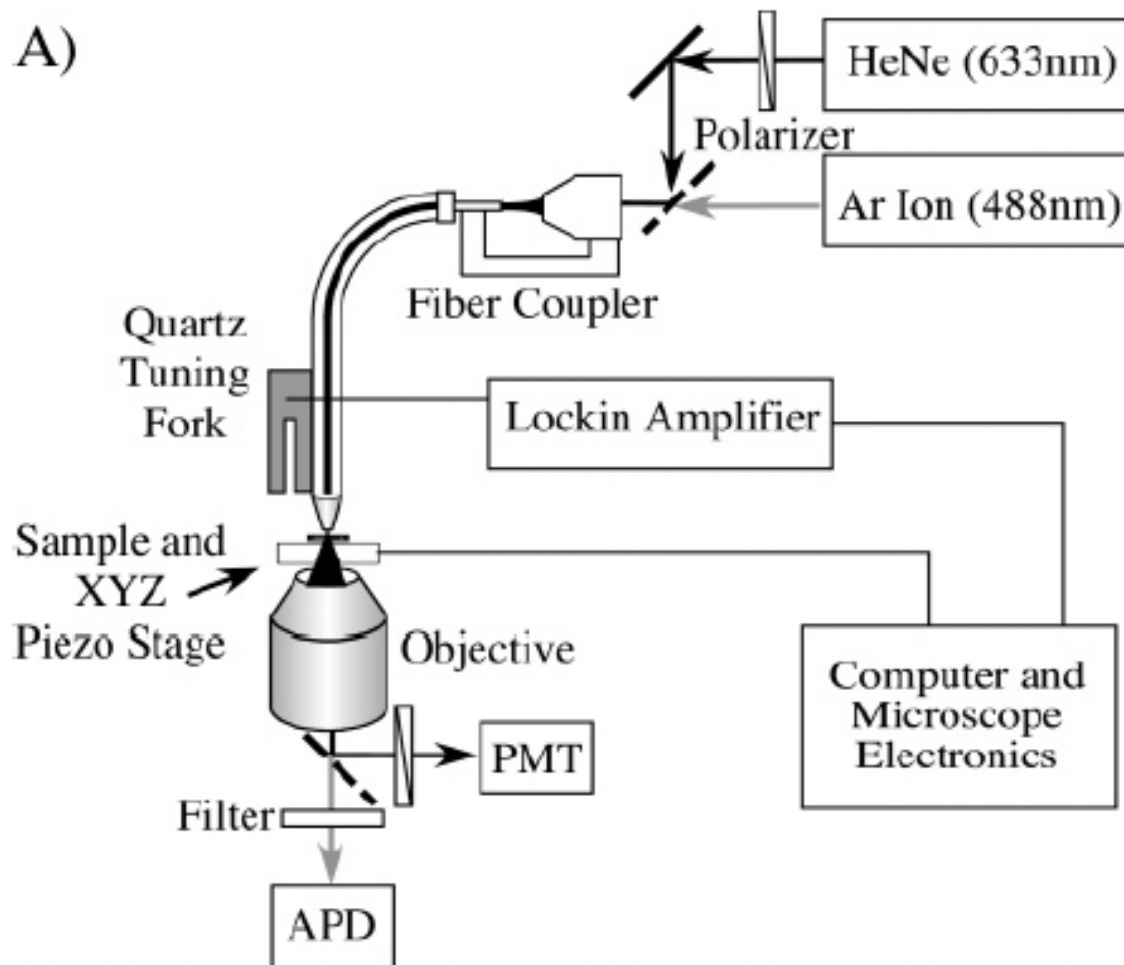


Polymer-dispersed liquid-crystal (PDLC) devices, along with others based on electrochromic technology, etc., have now been widely used in Smart Windows.

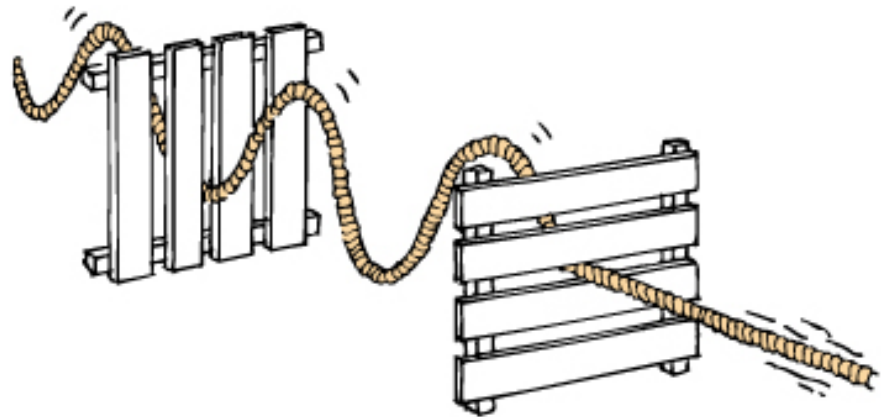
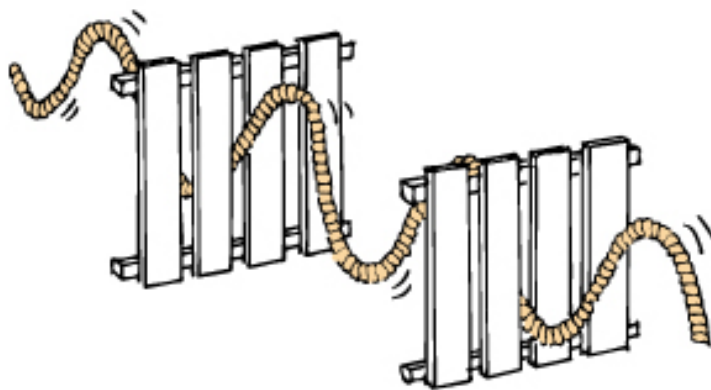
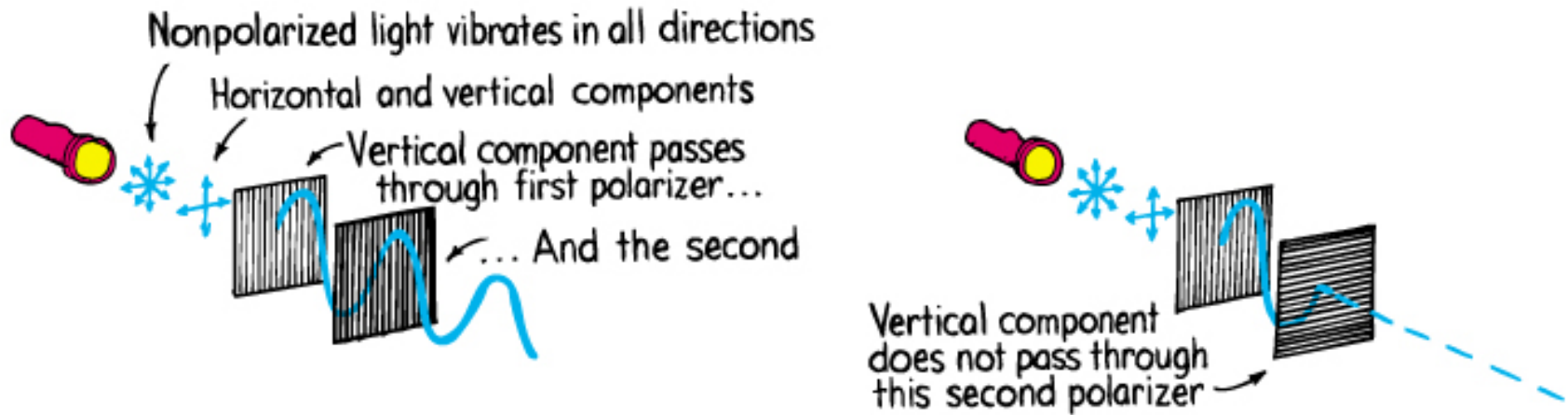
Electrochromic smart windows used in Dreamliner, Boeing 787



NSOM based on shear force mode



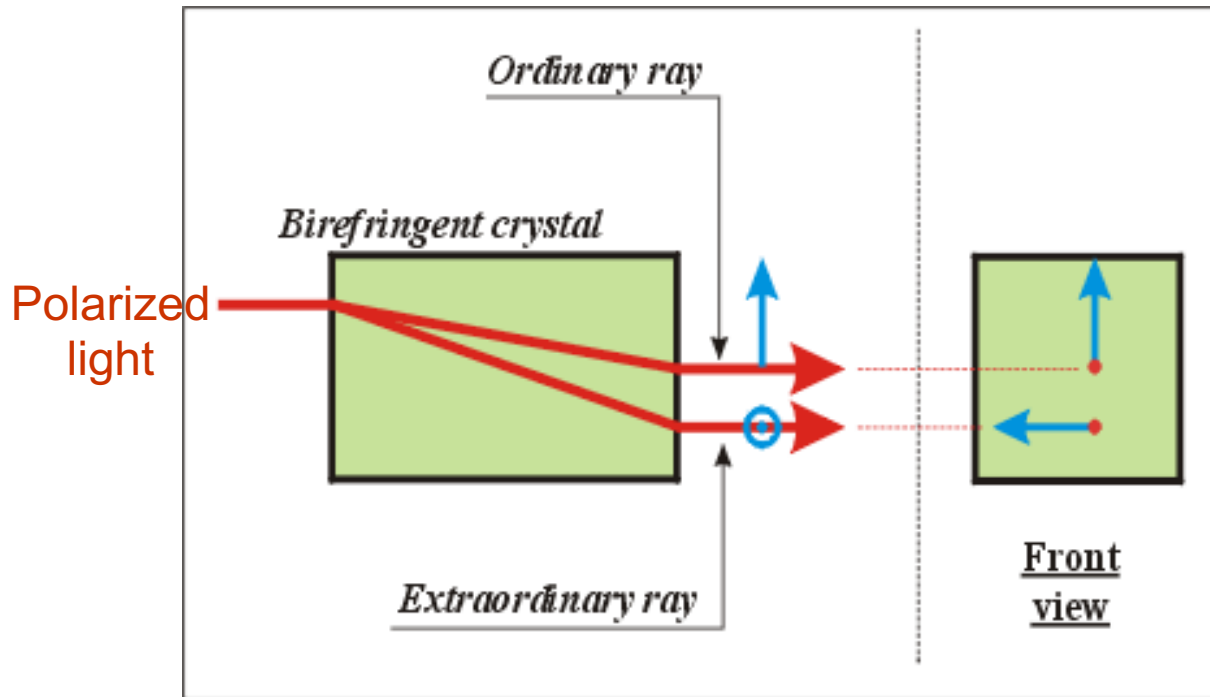
What is polarization?



Hewitt, *Conceptual Physics*, Ninth Edition.

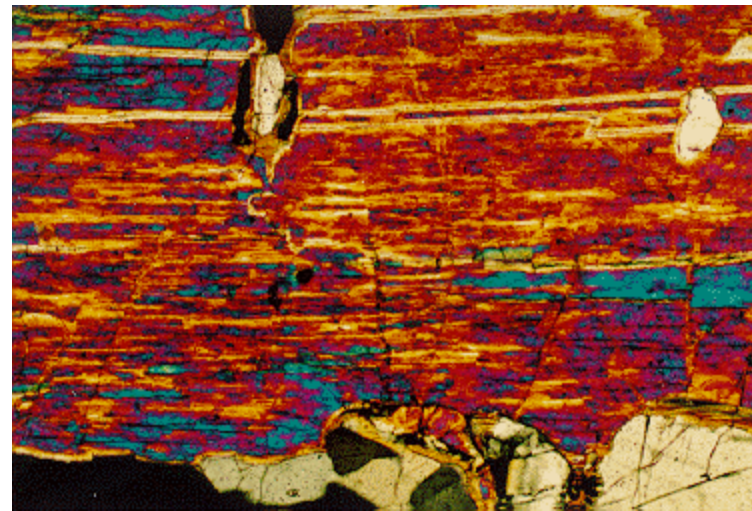
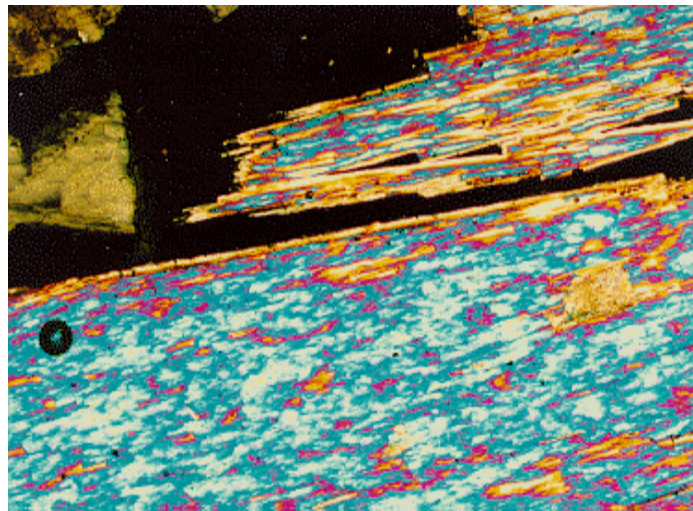
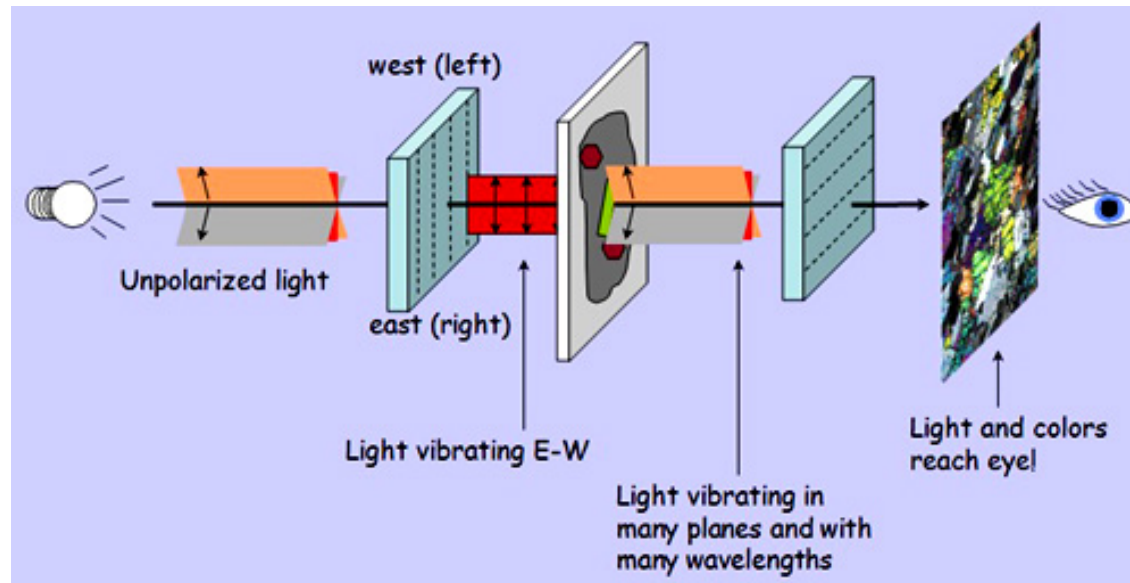
Copyright © 2002 Pearson Education, Inc., publishing as Addison Wesley. All rights reserved.

Birefringence

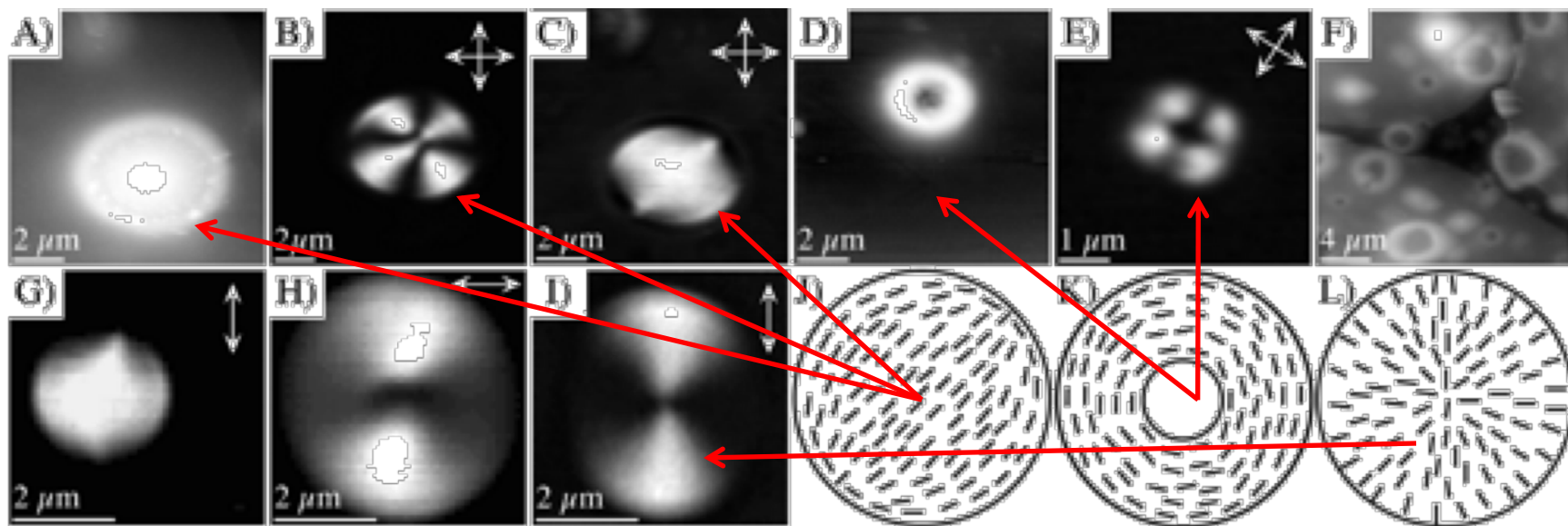


For isotropic materials, like glass, the polarization of the incident light remains the same.

Cross-polarized optical microscopy



thin section of tremolite under cross-polarized light



Images and models of several LC droplets. Panel A shows a topographic image of an ellipsoidal droplet. Panels B and C show NSOM birefringence images of two bipolar ellipsoidal droplets having optical axes oriented perpendicular and parallel to the film plane, respectively. Panel D shows a topographic image of a collapsed ("toroidal") droplet. Panel E shows the NSOM birefringence image of the droplet shown in panel D. Panel F shows a topographic image of a dye-doped PDLC sample showing several collapsed droplets. Panels G and H show multiphoton-excited fluorescence microscopy (MPEFM) images of bipolar and toroidal droplets, respectively. Panel I shows a MPEFM image of a PDLC droplet of radial configuration. Panels J-L show models for the LC organization in **bipolar, toroidal, and radial** droplets, respectively. Appended arrows show the incident and detected polarizations. MPEFM: multiphoton excited fluorescence microscopy

**Measuring Local Optical Properties: Near-Field Polarimetry
of Photonic Block Copolymer Morphology**

M. J. Fasaloka,^{*} Lori S. Goldner,[†] and J. Hwang

Optical Technology Division, National Institute of Standards and Technology, Gaithersburg, Maryland 20899-8441

A. M. Urbas, P. DeRege, T. Swager, and E. L. Thomas

*Departments of Materials Science and Engineering and Chemistry, Massachusetts Institute of Technology,
Cambridge, Massachusetts 02139*

(Received 11 July 2002; published 10 January 2003)

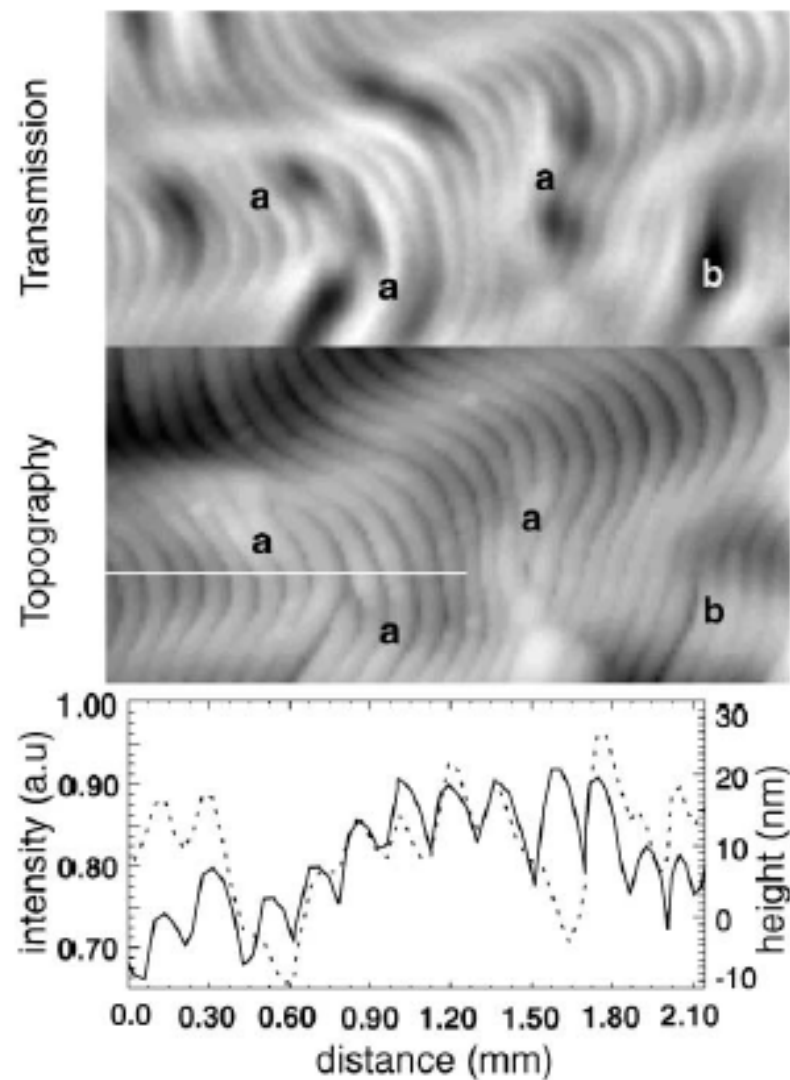


FIG. 1. NSOM images of PS-*b*-PI BC. Transmission (top), topography (middle). The plot (bottom) shows topography (solid) and transmission (dashed) along the white line (2.1 μm) in the topography image, smoothed over a three-pixel bin. Labels *a* and *b* show edge dislocations and lamellar separations, respectively.

Spatial Imaging of Singlet Energy Migration in Perylene Bis(phenethylimide) Thin Films**David M. Adams,^{†,§} Josef Kerimo,[‡] Donald B. O'Connor,[†] and Paul F. Barbara^{*,†}***Department of Chemistry and Biochemistry, University of Texas at Austin, Austin, Texas, 78712, and
Department of Chemistry, University of Minnesota, Minneapolis, Minnesota, 55455**Received: June 25, 1999; In Final Form: September 23, 1999*

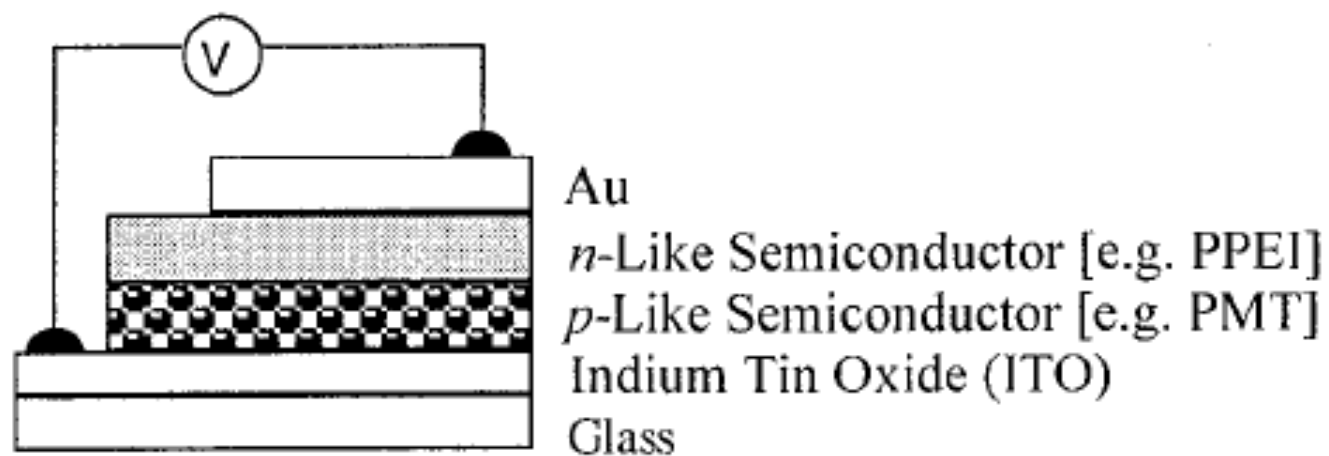


Figure 1. Schematic of typical organic semiconductor-based solar cell.

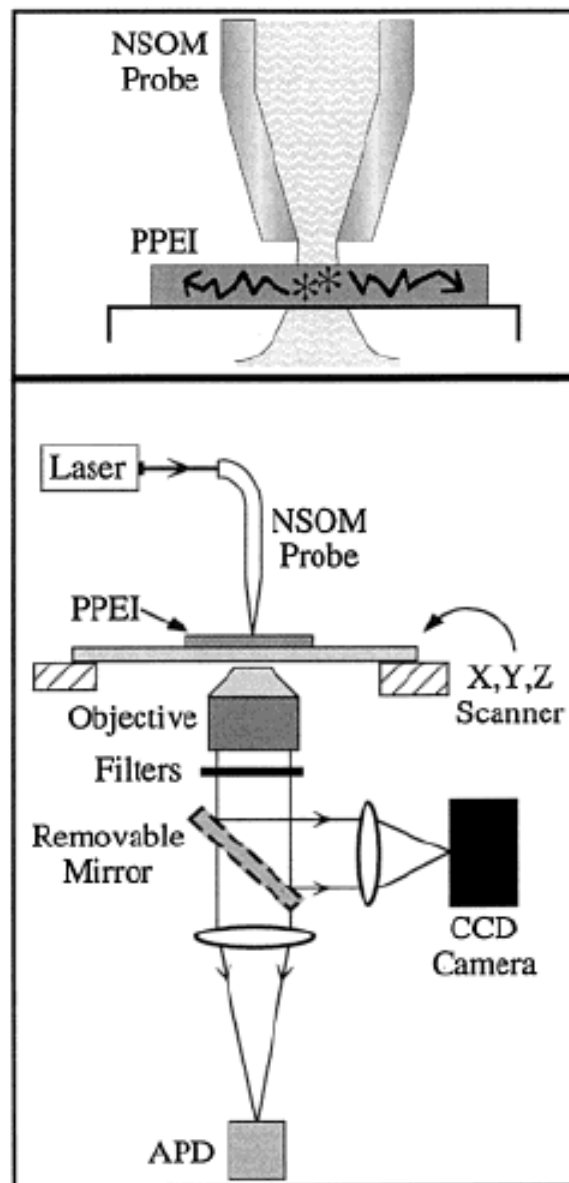


Figure 2. Experimental setup for far field/near field fluorescence imaging of PPEI microcrystals.

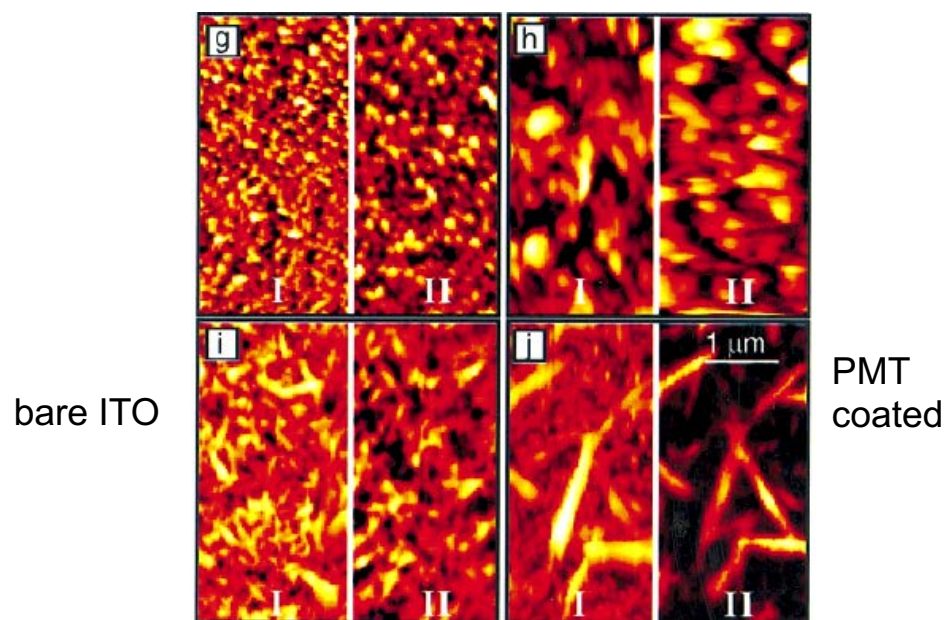
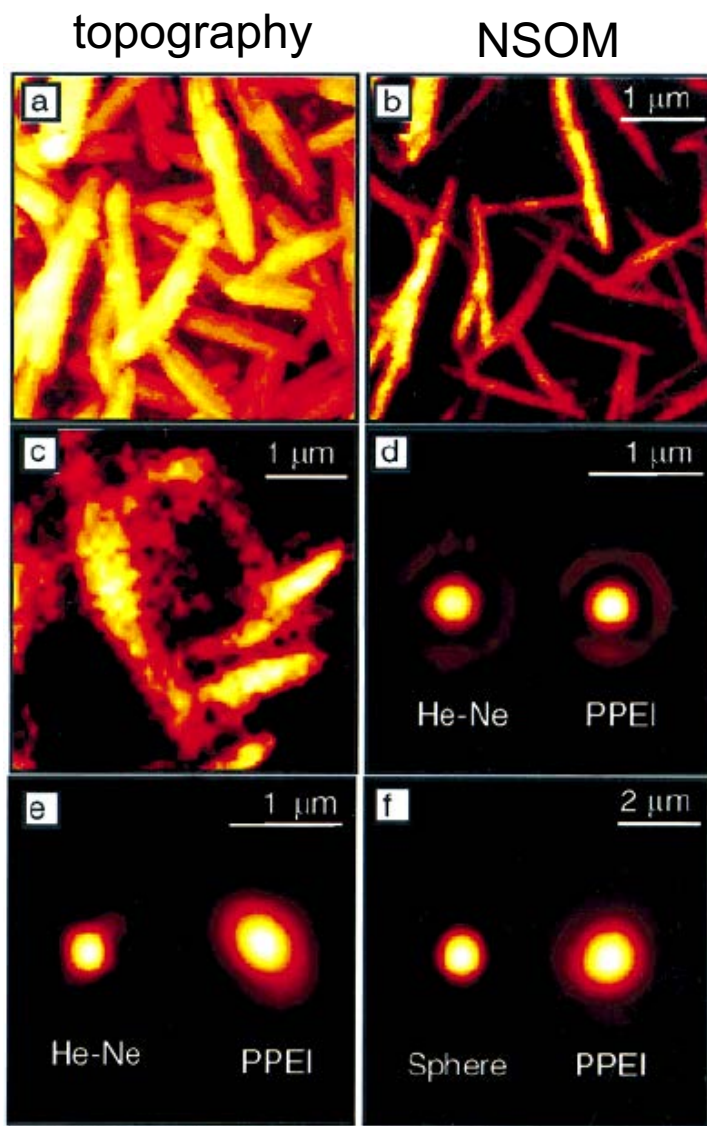


Figure 3. (a) Topography and (b) the simultaneously recorded near-field fluorescence image of PPEI microcrystals. (c) Far-field fluorescence imaging of PPEI microcrystals. Sample in (a–c) was solvent annealed extensively. (d) Spatial images of 633 nm HeNe laser from near field optical probe (left spot) and 680 nm emission (right spot) from a single PPEI microcrystal. (e) Spatial images of 633 nm HeNe laser (left spot) and 680 nm emission from a 150 nm thick PPEI film. (f) Spatial images of 680 nm emission from a 200 nm diameter fluorescent latex sphere (left spot) and a 50 nm thick PPEI film. (g) Topography of bare ITO and a PMT-coated ITO (I and II, respectively). (h) Topography of a 670 nm thick PPEI film on ITO and a 670 nm thick PPEI film on PMT-coated ITO (I and II, respectively). The samples were on the same underlying glass substrate and annealed under identical conditions. (i) Topography and fluorescence NSOM of a 24 nm thick PPEI film on bare ITO (I and II, respectively). (j) Topography and fluorescence NSOM of a 24 nm thick PPEI film on PMT-coated ITO (I and II, respectively). The samples in (i,j) were on the same underlying glass substrate and annealed under identical conditions. The scale is the same in (g–j). Images (a–d) were obtained with objective 1 and images (e–j) with objective 2.

Electric Field Modulated Near-Field Photo-Luminescence of Organic Thin Films

David M. Adams, Josef Kerimo, Chong-Yang Liu, Allen J. Bard, and Paul F. Barbara*

Department of Chemistry, University of Texas at Austin, Austin Texas 78712

Received: December 23, 1999; In Final Form: May 17, 2000

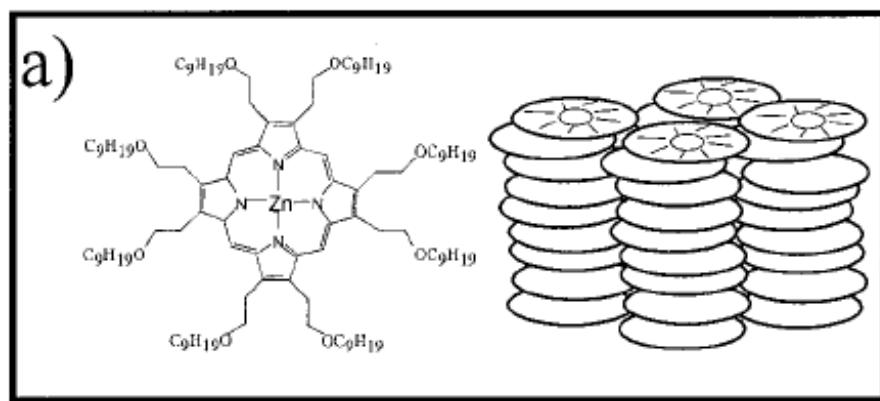
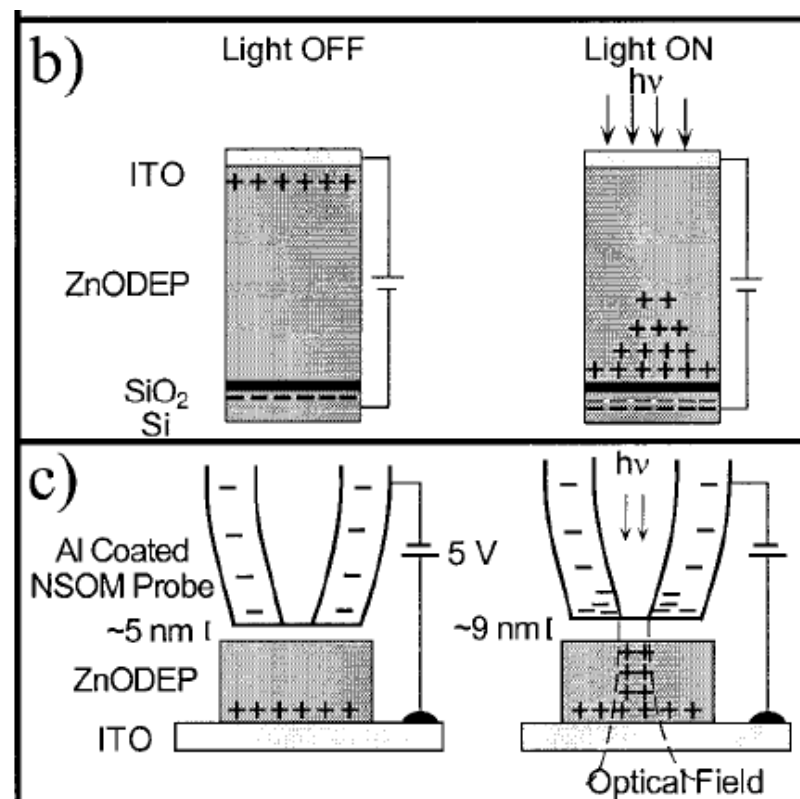
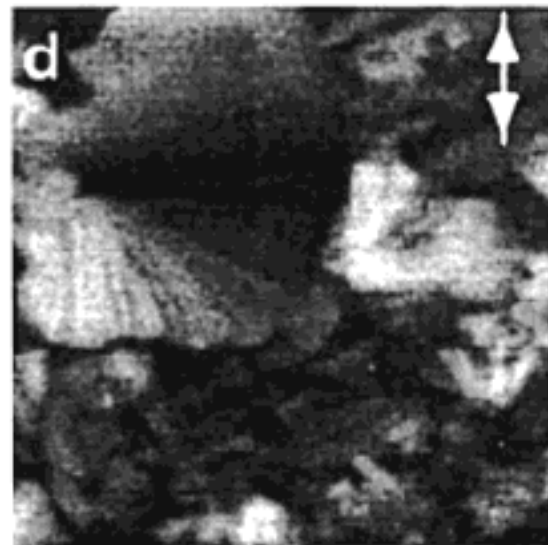
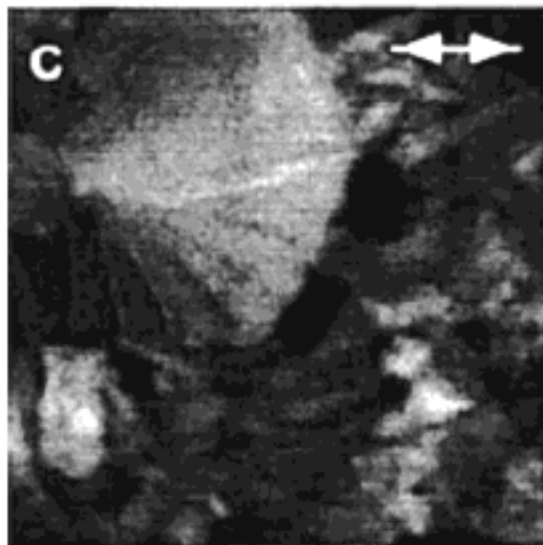
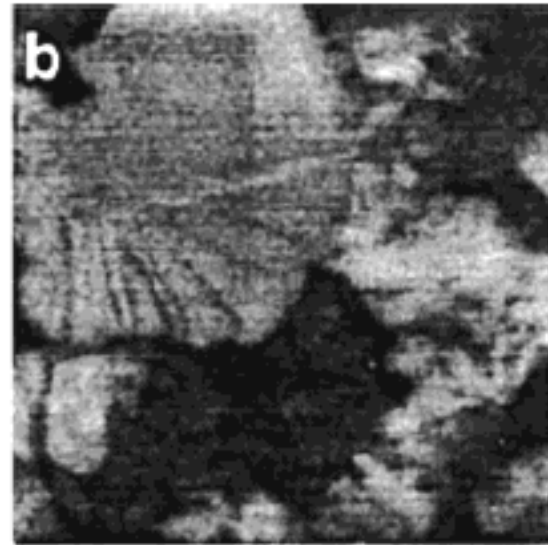
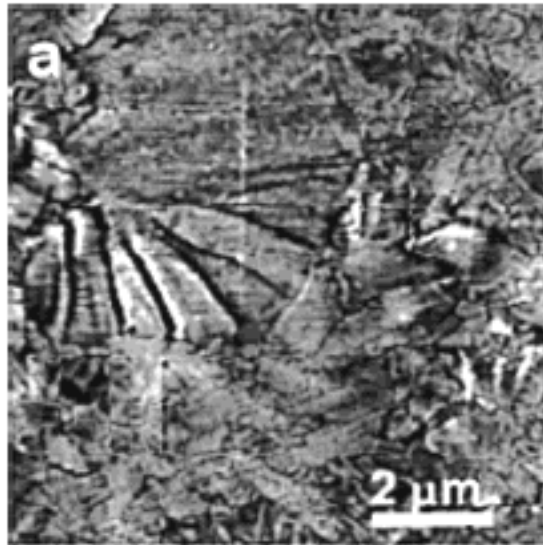


Figure 1. (a) Molecular structure of ZnODEP and proposed model of molecular stacking with some defects along the stacks. (b) Charge trapping photocapacitive device composed of ITO/ZnODEP/SiO₂/Si layer structure and proposed model of charging under illumination. (c) Device equivalent structure composed of ITO/ZnODEP/impurity-layer/Al-Coated Near-Field Probe.



Topographic

NSOM



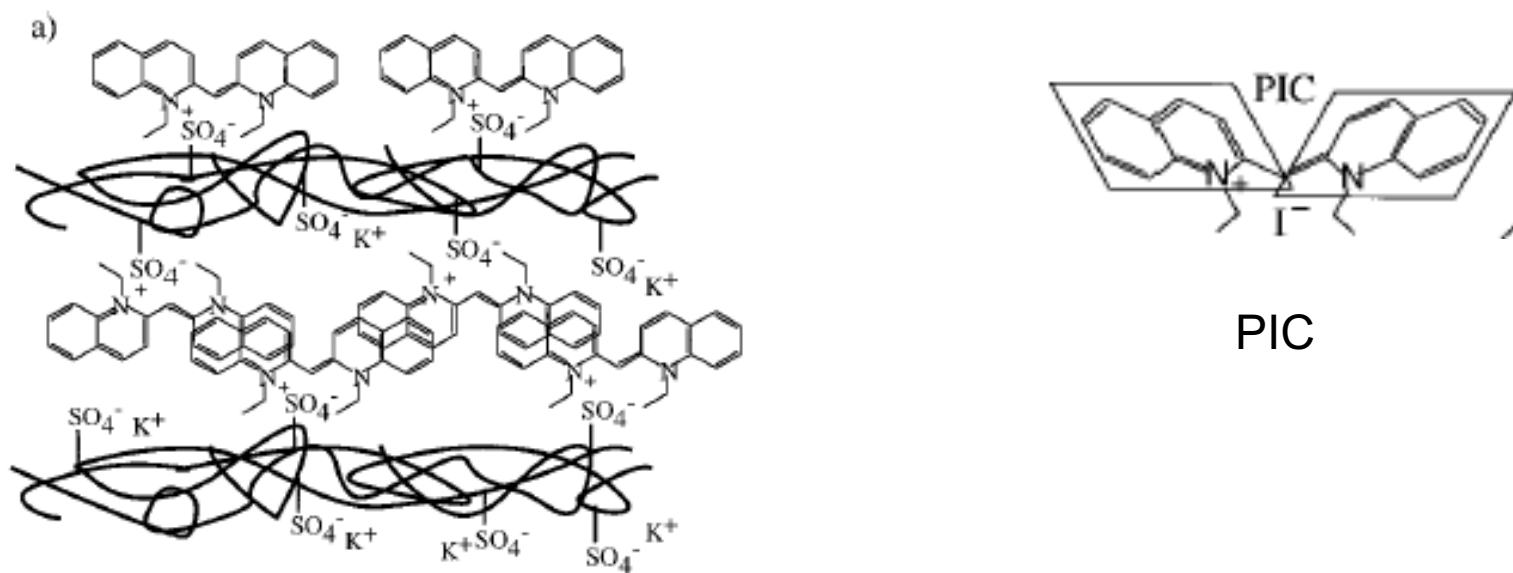
Polarized NSOM emission

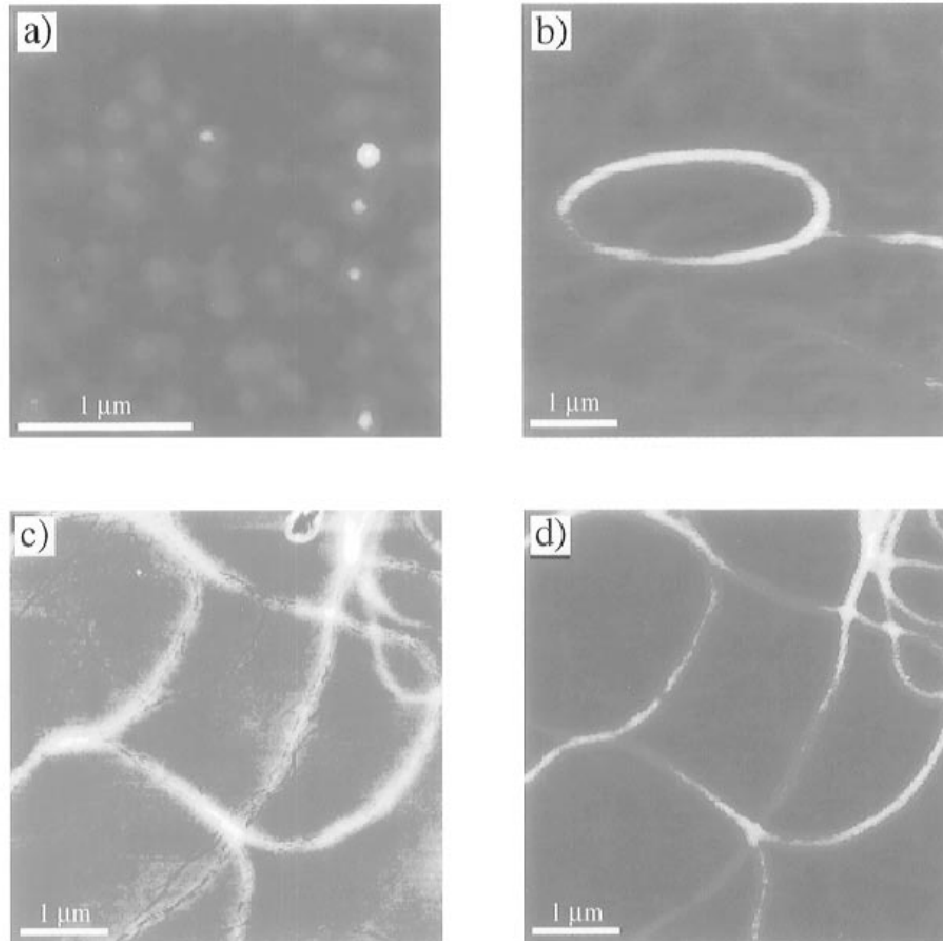
A Molecular Yarn: Near-Field Optical Studies of Self-Assembled, Flexible, Fluorescent Fibers

Daniel A. Higgins, Josef Kerimo, David A. Vanden Bout, and Paul F. Barbara*

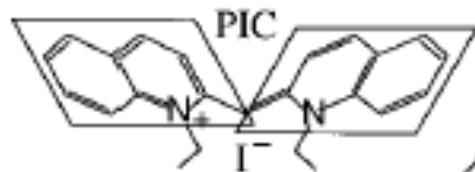
Contribution from the Department of Chemistry, University of Minnesota, 207 Pleasant Street SE, Minneapolis, Minnesota 55455

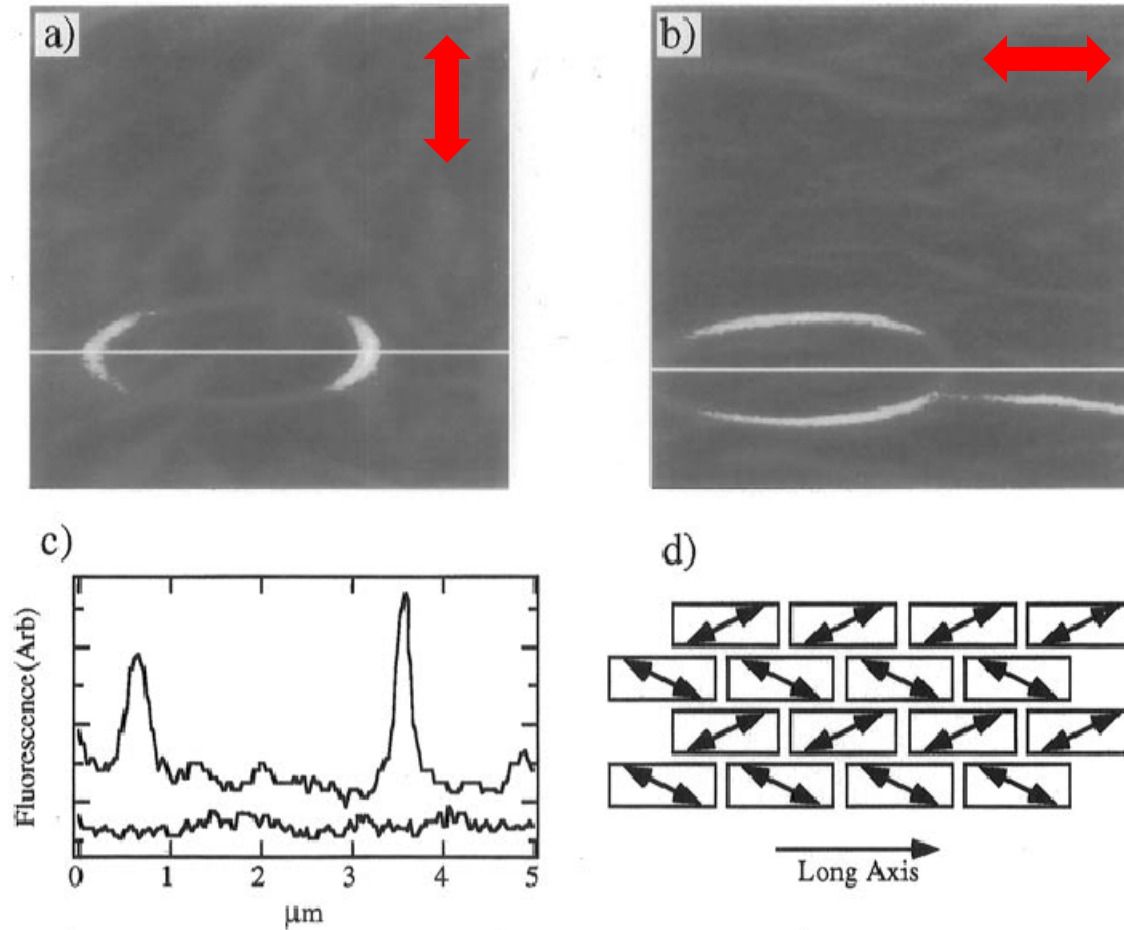
Received January 12, 1996[Ⓢ]





fluorescence NSOM images of a thin PVS film incorporating fluorescent fibers (PIC).





Polarization-dependent fluorescence near-field images of a ringlike fiber.

J|A|C|S

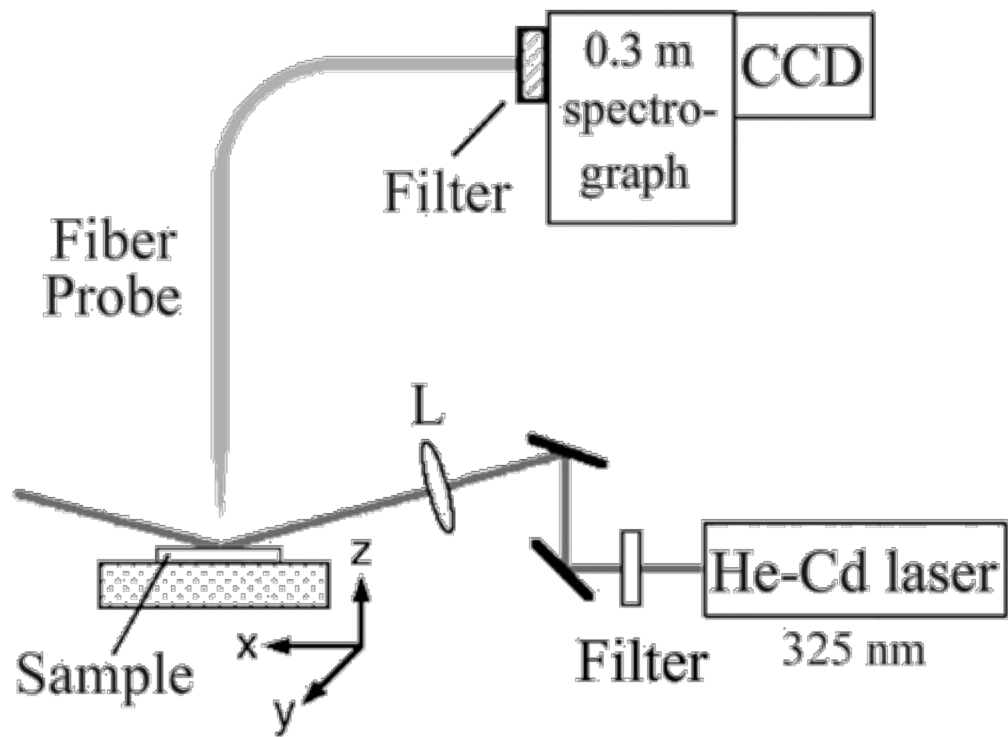
A R T I C L E S

Published on Web 11/27/2002

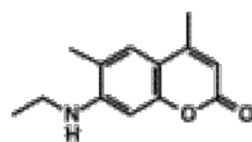
**Intermolecular Coupling in Nanometric Domains of
Light-Harvesting Dendrimer Films Studied by
Photoluminescence Near-Field Scanning Optical Microscopy
(PL NSOM)**

Lynn F. Lee, Alex Adronov,^{*,†} Richard D. Schaller, Jean M. J. Fréchet,^{*} and
Richard J. Saykally^{*}

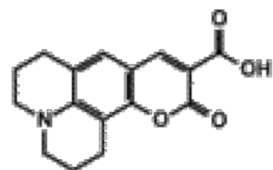
*Contribution from the Department of Chemistry, University of California,
Berkeley, California 94720*



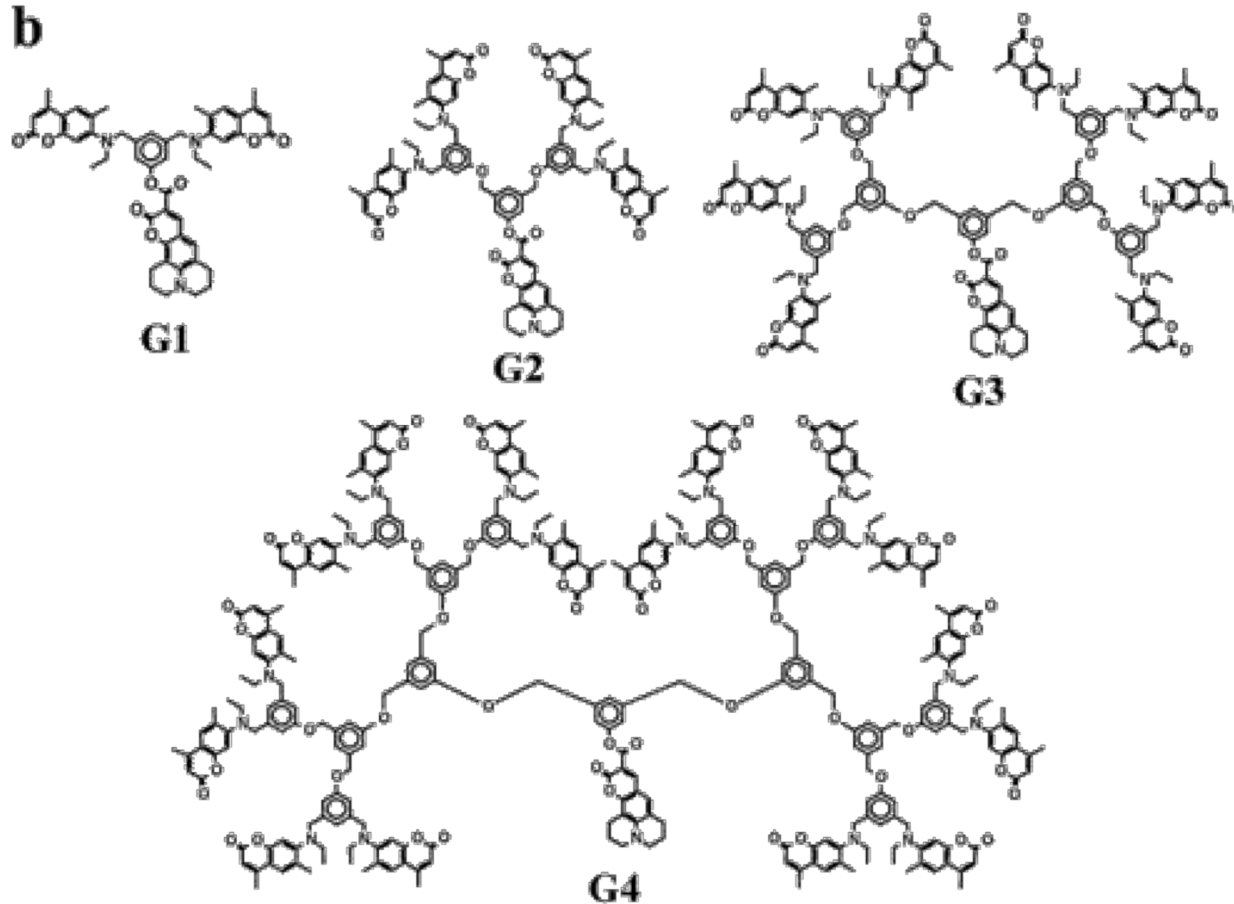
NSOM setup: tip collection

a

Coumarin 2
 $\lambda_{\text{max}} = 365 \text{ nm}$
 $\lambda_{\text{em}} = 435 \text{ nm}$

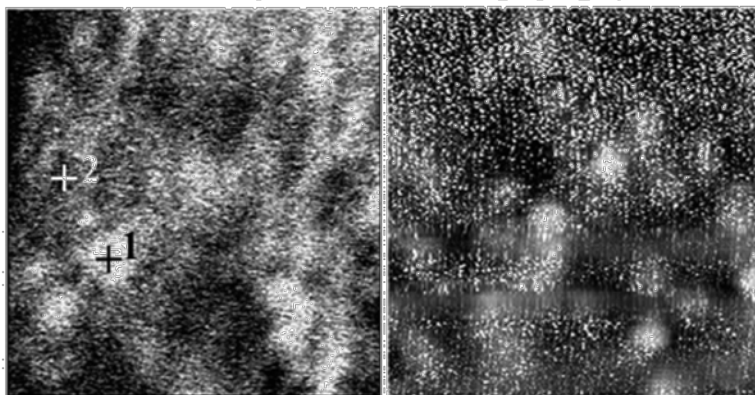


Coumarin 343
 $\lambda_{\text{max}} = 446 \text{ nm}$
 $\lambda_{\text{em}} = 490 \text{ nm}$

b

a. G1 NSOM image

b. G1 topography



a. G4 NSOM image

b. G4 topography

